# How close is the nearest node in a wireless network?

Amy L. L. Middleton[1], Antal A. Járai[2], Jonathan H. P. Dawes[3], and Keith Briggs[4]

[1,2,3]Dept. of Mathematical Sciences, University of Bath,
Claverton Down, Bath, BA2 7AY, United Kingdom.

[4]Applied Research, BT Technology, Adastral Park,
Martlesham Heath, IP5 3RE, United Kingdom

March 2, 2021

**Abstract**

The ability of small-cell wireless networks to self-organise is crucial for improving capacity and performance in modern communication networks. This paper considers one of the most basic questions: what is the expected distance to a cell's nearest neighbour in a spatially distributed network? We analyse a model problem in the asymptotic limit of large total received signal and compare the accuracy of different heuristics. We also analytically consider the effects of fading. Our analysis shows that the most naive heuristic systematically underestimates the distance to the nearest node; this is substantially corrected in cases of interest by inclusion of the next-order asymptotic term. We illustrate our theoretical results explicitly for several combinations of signal and path loss parameters, and show that our theory is well supported by numerical simulations.

Keywords: Wireless networks, femtocells, self-organising network, distance estimation, asymptotic approximation, Rayleigh fading

## 1 Introduction

The UK government Telecommunications Sector Report Parliament (2017) remarks that there is hardly a sector in the UK which does not rely in some shape or form on the connectivity provided by telecommunications, both in the services it enables, and the activities it supports. The report notes further that the failure of telecommunication systems, or the failure to invest in upgrading them to meet increasing demand, can have a direct negative impact on people's ability to do business and to interact socially. Not surprisingly, telecommunications are considered to be part of the UK's critical national infrastructure.

Rapid technological change and growing demands on the telecommunications sector have led to a focus on networks that are self-organising (SON) rather than centrally planned and controlled. SON is seen to offer many benefits: in energy and cost savings, improved network performance and better customer experience. In the UK, the need for self-organising networks has been brought sharply into focus with the first commercial market deployments of 5G in 2018. Associated with the deployment of 5G is the emergence of 'small-cell densification' (Deloitte, 2018). That is, small-cells will no longer just fill gaps; they will be essential to enabling 5G, particularly in densely populated areas . Dense small-cell networks with large numbers of devices will require better self-organising

1

properties in order to provide the robustness and resilience that society expects from critical national infrastructure; SON will have significant impact and benefit. Looking globally, annual growth in investments in SON technology is expected to be around 11% between 2019 and 2022 (SNS Telecom & IT, 2018); it has been estimated that SON will account for a market worth \$5.5 bn by 2022.

This paper supports the above technological ambitions for SON by asking a seemingly simple question ('How close is the nearest node?') that applies to any set of transmitting devices distributed randomly in the plane. The main applications that we have in mind are cellular systems such as current 4G or future 5G networks. Each cell includes a fixed-location transceiver (generically referred to as a base station) capable of wireless connection to individual user devices. Together the cells provide coverage over larger geographical areas than could be covered by a traditional single large transmitter (a macrocell base station, or MBS). The current trend for higher and higher densities of cells necessitates better self-organisation of these networks, but results in benefits such as increased capacity and reduced power consumption for individual user devices.

Low power cellular base stations are often referred to as 'femtocells'; these are similar to home wi-fi hubs, are relatively inexpensive and can overlay an existing cellular network. Femtocells provide 4G, and will eventually provide 5G, coverage to user devices hence allowing for better network capacity and coverage in areas where it is currently poor or absent (Cheung et al., 2012; Vaz et al., 2013). Networks employing femtocells take advantage of the fact that more than 50% of all voice calls and more than 70% of data traffic originates indoors. Femtocells backhaul data through a broadband gateway over the internet and their deployment could efficiently relieve indoor traffic from expensive MBSs, freeing up MBSs to handle communications traffic from truly mobile users and giving those other parts of the network higher capacity (Lan et al., 2010; Cheung et al., 2012).

In addition to capacity and coverage questions, new networks change the planning behind the spatial distribution of transmitters. Traditionally, MBSs were sited by the communications firm after a geographically based planning exercise. The location and configuration settings of the MBS were chosen to optimise the network's performance. In contrast, femtocells are placed by end users (Carle et al., 2013), their locations are largely unplanned, and optimal configuration settings cannot be computed in advance. Hence the need for self-optimising, self-organising networks. To be precise, the term 'self-organising' is used to mean that the network is (i) self-optimising and (ii) self-diagnosing (Tall et al., 2014). A *self-optimising* network is one where the cells in the network choose configuration settings which optimise the global network performance. To be *self-diagnosing* the network needs to have the ability to detect and adapt to change, such as the removal or addition of a cell, so that network performance is still maintained and, indeed, optimised. A third element commonly referred to in SON is the ability of a cell to be initially self-configuring; this is sometimes referred to as a 'plug-and-play' capability.

Network performance is evaluated quantitatively by measuring the quality of the connections between transmitters and their paired user devices; by 'paired' we mean the devices which transmit to, and receive from, the relevant transmitter. Since transmitters broadcast indiscriminately, a user device receives signal $S$ from its paired transmitter as well as signals from all non-paired transmitters, now considered as interference, $I$.

Neglecting noise, the connection quality can be characterised by the Signal to Interference Ratio (SIR), the higher the better. This then potentially drives an instability: in order to increase SIR for its paired user devices, a transmitter could simply increase its signal strength. However, since a transmitter will only be aware of the SIR corresponding to its own paired user devices, this behaviour would be highly likely to result in increased interference between other transmitters and their paired devices, and hence this behaviour would lower the SIR elsewhere in the network, resulting in lower overall network performance.

Figure 1 illustrates a case in which a transmitter (A) is using a signal strength that is higher
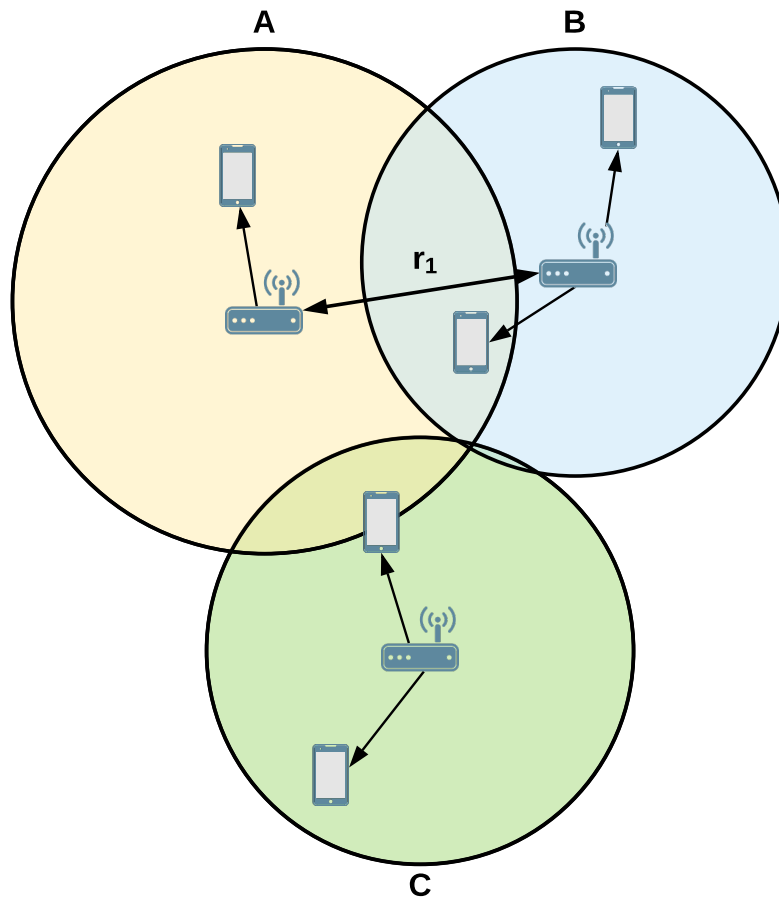
Figure 1: An example of a non-optimal configuration for a self-organising network consisting of three transmitters A, B and C and a collection of user devices. Pairings between transmitters and devices are indicated by the (single-headed) arrows. The coloured circles illustrate the effective coverage of each transmitter. User devices in the overlaps between circles A∩B and A∩C are paried with B and C respectively, and so will have non-optimal SIRs due to interference from A. Reducing the signal strength of transmitter A would improve the SIR for those devices and the need for such a reduction could be informed by good estimation of the distance $r_1$ between A and its nearest neighbour transmitter (B).

than optimal for the network. In Figure 1, the requirement for A to reduce its signal strength can be better judged if the distance from A to its nearest neighbour (in this case B) can be estimated accurately. The difficulty though is that the total interference reported to A by its paired devices is a sum of signal strengths: those of transmitters B and C combined.

Since the priority in network performance is to provide a good minimum standard of service, monitoring the minimum SIR in the network usually takes priority over achieving a high SIR for a minority of devices. However, achieving this in practice is of course complicated by a lack of available information about the local network, and hence the requirement for distributed self-organisation, without direct or indirect communication via a central node. Learning about the spatial distribution of other transmitters, via the interference reported by paired user devices, is therefore a cruicial feature allowing transmitters in self-organising networks to adjust their power levels in order to optimise SIR across the network as a whole. Within this framework, the correct estimation of the distance from a transmitter to its nearest neighbour, becomes a key question, and the one we address here.

## 1.1 Mathematical formulation of the problem and the main result

Mathematical models of the real world are always simplifications. In the case at hand our major simplifications are that we make assumptions about the distribution of cells, the relationship between distance and signal, and the effects of fading in the network. This section outlines these assumptions and their justifications, and presents the main results of the paper.

Each femtocell (transmitter) in the network transmits a signal to be received by user devices. The strength of the signal received is determined by the separation distance and transmission strength. Path-loss is the term used to describe the reduction in signal strength (or power density) in an electromagnetic wave which results from propagation along a particular path through space. Losses increase with distance travelled but the exact relationship between path-loss and distance depends on the medium. Approximations for path-loss fall broadly into two categories: over short distances the path-loss is termed 'near-field', while at longer distances the path-loss is termed 'far-field'. In the simplest cases, near-field path-loss is attenuation by just a constant factor, while in the far-field case the received signal strength is modelled as a power law. For reasons of analytical convenience, we here assume that all path-loss is far-field. This is in fact a common approach, used by many authors, for example Sousa & Silvester (1990), Win et al. (2009) and Lichte et al. (2010). More precisely, let $r$ be the distance between the femtocell and the user device, and $\gamma$ be the path-loss exponent, then in the far-field case the received signal power $S \propto r^{-\gamma}$. For mathematical reasons we always assume that $\gamma > 2$: the value $\gamma = 4$ is commonly used in the literature.

Signal strength falls for reasons other than distance, for example reflection or diffraction due to obstacles. The term *propagation effects* is generally used to describe these. In this paper we conside one particular propagation effect, known as *fading*.

Fading arises due to the multiple paths taken by signals between transmitter and receiver; 'multi-path reception' describes the situation where the signal offered to the receiver contains the direct 'line of sight' wave as well as a large number of reflected waves. Fading refers to the reduction in signal strength that is caused when reflected waves interfere with the direct wave. Without detailed knowledge of the environment, one must reply on models for the typical effect of fading on signal strength. We consider a widely-used model for fading, appropriate to wireless radio networks of the kind that motivated this work, known as Rayleigh fading. Rayleigh fading rests on a number of assumptions, for example that a multi-path received signal consists of a large number of reflected waves which are independent and identically distributed. Mathematically, the effect of Rayleigh fading on a signal received from a single source is to multiply the anticipated strength $S = r^{-\gamma}$

(ignoring a constant of proportionality) by a (suitably normalised) exponentially-distributed random variable $H$, i.e. we assume that $H$ is $\mathsf{Exp}(1)$ distributed. Hence the received signal after fading is now a random variable $T = H r^{-\gamma}$.

Rayleigh fading is a special case of Nakagami-$m$ fading, in which the multiplicative random variable is $\Gamma(m, 1/m)$ distributed. Nakagami-$m$ fading attempts to take into account that multiple propagation paths may also contain contributions from signals of different strengths. The case of Rayleigh fading is recovered when $m = 1$. When $m > 1$ the fluctuations in signal strength are reduced due to the more peaked nature of the Nakagami-$m$ distribution; in some sense the Rayleigh fading case has the most extreme effect on the strength of the received signal.

The spatial configuration of transmitters and receivers is of course critical in determining the performance of the wireless network. A stochastic model for node locations (i.e., a spatial point process) is needed. In situations where nodes are located randomly over a large area, the analytical tractability of the homogeneous Poisson point process (PPP) has made it the most widely used model Haenggi (2012). The paper by Andrews et al. (2010), favourably compares typical realisations of a PPP to base station deployment in urban areas. Analytical tractability is a key consideration in mathematical modelling problems, hence as a first case we choose the PPP, leaving consideration of other point processes such as the Matérn or Ginibre processes (Deng et al., 2015; Kong et al, 2018), to be studied in future work.

A realisation of a Poisson point process is most easily described as a random collection of points in $\mathbb{R}^2$ in which the number of points in a given area $A$ is Poisson distributed, i.e. according to the $\mathsf{Poisson}(\lambda A)$ distribution, such that the numbers of points in any pair of disjoint subsets of the plane are independent. We represent the distribution of transmitters as points in $\mathbb{R}^2$ distributed according to a Poisson point process with intensity $\lambda$, and we imagine being stationed at the origin and measuring the total broadcast signal strength that is received there. This total signal is now a random variable $S$, taking values for specific realisations that we denote by $s$.

First, ignoring fading, the question now becomes: given that signal strengths reduce (hopefully rapidly) with distance, what is the expected error in attributing $S$ entirely to the nearest transmitter? That is, if $R_1$ is the distance from the origin to the nearest transmitter, what is the expected error in estimating $R_1$ by $s^{-1/\gamma}$? Our main result is that the error in this naive approximation is, in the limit of large $s$, asymptotic to

$$\frac{2\,\lambda\,\pi}{\gamma}\, a(\gamma)\, s^{-3/\gamma}, \quad \text{as } s \to \infty, \tag{1}$$

where the constant $a(\gamma)$ is given explicitly in terms of hypergeometric functions. Our computations agree with numerical simulations which show that even for moderate values of $s$ the accuracy of (1) is considerably greater than that of the naive approximation. Since (1) is positive, the answer to the question posed in the title of the paper is that the nearest node is slightly further away than you would expect from the naive approximation $s^{-1/\gamma}$, i.e. that $s^{-1/\gamma}$ is systematically an underestimate of the distance to the nearest node.

Second, in the case with fading, if the observed total signal $T$ takes the value $t$ then a simple heuristic would be to use $(ct)^{-1/\gamma}$ where $c$ is a scaling factor which makes $cT$ have the same distribution as $S$ (the signal without fading). We propose an improvement on this which is in fact an approximate probability distribution of $R_1$ depending on the measured value $T = t$. The approximate conditional probability density for $R_1$ is given by

$$f_{R_1 \mid T}(r_1 \mid t) \approx \frac{1}{Z(t, \gamma, \lambda)} r_1^{\gamma+1}\, e^{-t\, r_1^{\gamma}}, \quad 0 < r_1 < (\lambda \pi)^{-1/2},$$

where the normalization $Z$ can be expressed in terms of the lower incomplete Gamma function. We

show that this is a considerable quantitative improvement and, being a distribution, provides more information than the simple rescaling heuristic.

## 1.2 Structure of the paper

First, in section 2, we consider the case without fading. We compute an asymptotic approximation to estimate the distance to the nearest transmitter. Subsection 2.2 gives an illustrative example, focussing on the case in which there are exactly three transmitters in the disk of radius 1 around the origin, and the path loss exponent is $\gamma = 4$. We focus on the case of three transmitters since this is the simplest case where all the necessary ideas can be demonstrated. Then, in subsection 2.3 we provide an overview of the computations for the general case in which there are $k$ transmitters in a disk of radius $\rho$ around the origin and the path loss exponent $\gamma$ is arbitrary. One part of the calculation is particularly tedious and so these computations are relegated to Appendix A. In subsection 2.4 we complete the derivation of the main result for the case with no fading by summing over the number of transmitters $k$.

In section 3, we compare our asymptotic formula against numerical simulations. We then introduce fading in section 4, where we devise and compare new heuristics for this case. As before, we compare our theoretical results with numerical simulations in subsection 4.3. A summary and conclusions are given in section 5.

## 2 Asymptotic Heuristic

In the limit of large total signal strength $s$ the naive heuristic $R_1 \approx s^{-\frac{1}{\gamma}}$ is appropriate since in this limit the total signal is likely to be dominated by the contribution from the closest transmitter. We therefore frame the asymptotic analysis as estimating the error in the naive heuristic. After a few preliminaries, we outline the derivation in the case of general $\gamma > 2$ in subsections 2.3 and 2.4. Details are given in Appendix A.

## 2.1 Preliminaries

Let $0 < R_1 < R_2 < \ldots$ denote the distances of the Poisson points from the origin taken in increasing order. Then $S = \sum_{i \geq 1} R_i^{-\gamma}$ (this sum converges with probability 1 as long as $\gamma > 2$). We condition on a measured signal value $S = s$. Then $R_1 \geq s^{-1/\gamma}$ always, and heuristically, $s^{-1/\gamma}$ should be a good approximation of $R_1$, at least if $s$ is not small, as argued by Webster (2015). We are interested in the expectation of the error, i.e. $\mathbf{E}\big[R_1 - s^{-1/\gamma} \,\big|\, S = s\big]$, as $s \to \infty$.

It will make computations easier to split $S$ into a sum of two terms as follows. Fix a constant radius $0 < \rho < \infty$, and let $N$ be the number of transmitters (Poisson points) inside the disk of radius $\rho$ centred at the origin. Note that $N$ is $\mathsf{Poisson}(\lambda \pi \rho^2)$ distributed. Write $S = S' + \bar{S}$, where $S' = \sum_{i=1}^{N} R_i^{-\gamma}$ is the contribution of transmitters within radius $\rho$, and $\bar{S}$ is the contribution of all other transmitters. Note that $\bar{S}$ can be neglected in the limit $s \gg 1$. This is because $\bar{S} = O(1)$, with an exponentially fast decaying probability tail as can be seen from the fact that its Laplace transform is finite in a neighbourhood of 0. Therefore, for large $s$, it is equivalent to consider $S$ and $S'$. This argument is further supported by the fact that we find

$$\mathbf{E}\Big[R_1 - s^{-1/\gamma} \,\Big|\, S' = s\Big] \sim \frac{2\lambda\pi}{\gamma}\, a(\gamma)\, s^{-3/\gamma}, \quad \text{as } s \to \infty, \tag{2}$$

holds *independent* of the chosen value of $\rho$ (that is, only the error of the asymptotics depends on

$\rho$). The coefficient $a(\gamma)$ is computed explicitly to be

$$a(\gamma) = \gamma\, 2^{(2-\gamma)/\gamma}\left[\,{}_2F_1\left(\frac{\gamma+2}{\gamma}, -\frac{2}{\gamma}; \frac{\gamma-2}{\gamma}; \frac{1}{2}\right) - {}_2F_1\left(\frac{\gamma+3}{\gamma}, -\frac{2}{\gamma}; \frac{\gamma-2}{\gamma}; \frac{1}{2}\right)\right], \quad \gamma > 2, \quad (3)$$

where the hypergeometric series is given by ${}_2F_1(a, b; c; z) = \sum_{n=0}^{\infty} \frac{(a)_n (b)_n}{(c)_n} \frac{z^n}{n!}$ with $(q)_n = q(q+1)...(q+n-1)$.

The following asymptotic result is derived in section 2.3, with some details deferred to Appendix A:

$$\mathbf{E}\left[R_1 - s^{-1/\gamma} \,\middle|\, S' = s,\, N = k\right] \sim \frac{2\,(k-1)\,\rho^{-2}}{\gamma}\, a(\gamma)\, s^{-3/\gamma}, \quad \text{as } s \to \infty, \text{ for } k \geq 1,\, 0 < \rho < \infty. \quad (4)$$

Following this, we argue that the conditional distribution of $N$ given $S' = s$ satisfies

$$\mathbf{P}[N = k \mid S' = s] \sim e^{-\lambda\pi\rho^2} \frac{(\lambda\pi\rho^2)^{k-1}}{(k-1)!}, \quad \text{as } s \to \infty, \text{ for } k \geq 1,\, 0 < \rho < \infty. \quad (5)$$

Finally, multiplying (4) by (5) and summing over $k = 1, 2, \dots$ to remove the conditioning on $N$ yields the expression in the right hand side of (2). This last step is set out in section 2.4.

Before delving into the details of the computations, we comment on the probabilistic insight behind them. Since $S'$ can be represented as the sum of $N$ independent heavy-tailed random variables, the most likely way a large value $S' = s$ results, is that the largest of them, $R_1^{-\gamma}$, dominates the sum, while the remaining terms take on 'typical' values (as if unconditioned). This has the consequence that $N - 1$, the number of *extra* transmitters (different from the nearest) will be approximately $\mathsf{Poisson}(\lambda\pi\rho^2)$ distributed. Let us write

$$R_1 - s^{-1/\gamma} = \left(s - R_2^{-\gamma} - \cdots - R_N^{-\gamma}\right)^{-1/\gamma} - s^{-1/\gamma} = s^{-1/\gamma}\left[\left(1 - \frac{R_2^{-\gamma}}{s} - \cdots - \frac{R_N^{-\gamma}}{s}\right)^{-1/\gamma} - 1\right]. \quad (6)$$

Due to the observation above about $R_1^{-\gamma}$ dominating, the right hand side should be approximately

$$s^{-1/\gamma}\, \mathbf{E}[N - 1 \mid S' = s]\, \mathbf{E}\left[\left(1 - \frac{R_2^{-\gamma}}{s}\right)^{-1/\gamma} - 1 \,\middle|\, S' = s, N = 2\right]. \quad (7)$$

Here the first expectation is $\approx \lambda\pi\rho^2$, and the conditional expectation can be determined from the integral

$$\int_{(\frac{1}{2}s)^{-1/\gamma}}^{\rho}\left[\left(1 - \frac{r^{-\gamma}}{s}\right)^{-1/\gamma} - 1\right] r\, dr = \frac{s^{-2/\gamma}\rho^{-2}}{\gamma}\int_{\rho^{-\gamma}/s}^{1/2} \frac{(1-y)^{-1/\gamma} - 1}{y^{1+2/\gamma}}\, dy \sim s^{-2/\gamma}\, \rho^{-2}\, \frac{a(\gamma)}{\gamma}.$$

Putting the above heuristics together yields the right hand side of (2). However, we have not found a simple probabilistic proof to make the connection between (6) and (7), and therefore we instead compute the relevant integrals. This has the added benefit that it yields an error estimate for the asymptotics in (4).

## 2.2 Example: computations in the case $N = k = 3$, $\gamma = 4$

To illustrate the calculations in the general case, we first examine the case $k = 3$ as an example. This case demonstrates all the methods used for larger $k$ (which $k = 2$ does not), and hence is the shortest non-trivial example. Observe that when $N = k = 1$ and $S' = s$, then $R_1 = s^{-1/\gamma}$, so (4) holds trivially. (Clearly $N = k = 0$ is impossible when $S' = s > 0$).

For Poisson distributed points, the probability density of having three points in a disk of radius $\rho = 1$ at radii $r_1, r_2, r_3$ is

$$f_{R_1, R_2, R_3, N=3}(r_1, r_2, r_3) = (2\lambda\pi)^3 e^{-\lambda\pi} r_1 r_2 r_3, \quad \text{where} \quad 0 < r_1 < r_2 < r_3 < 1.$$

Since by assumption $\gamma = 4$ and there is no fading, the radii $r_i$ and signal strengths at the origin $s_i$ are related by $r_i = s_i^{-1/4}$ which implies $|dr_i/ds_i| = (1/4)s_i^{-5/4}$. Substituting these expressions allows us to determine a probability density in terms of signal strengths rather than distances:

$$f_{S_1, S_2, S_3, N=3}(s_1, s_2, s_3) = e^{-\lambda\pi}(2\lambda\pi)^3 (1/4)^3 s_1^{-3/2} s_2^{-3/2} s_3^{-3/2}, \quad \text{where} \quad 1 < s_3 < s_2 < s_1 < \infty.$$

Conditioning on the total signal $S' = s = S_1 + S_2 + S_3$ (as well as on $N = 3$ which we assumed from the beginning), and expressing $S_1 = s - S_2 - S_3$ gives

$$f_{S_2, S_3 \mid N=3, S'=s}(s_2, s_3 \mid s) = \frac{1}{Z_{3,s}}(s - s_2 - s_3)^{-3/2} s_2^{-3/2} s_3^{-3/2}, \quad \text{where} \quad 1 < s_3 < s_2,$$

where the normalizing constant is

$$Z_{k=3,s} = \int_1^{s/3} ds_3 \int_{s_3}^{(s-s_3)/2} ds_2 \, (s - s_2 - s_3)^{-3/2} s_2^{-3/2} s_3^{-3/2}.$$

The limits on the integrands come from the inequality $s_1 > s_2 > s_3 > 1$ and the assumption $s_1 + s_2 + s_3 = s$.

The expectation of the error in the naive heuristic, in the case where $k = 3$, can therefore be written as

$$\mathbf{E}\left[R_1 - s^{-1/4} \,\middle|\, N = 3, \; S_1 + S_2 + S_3 = s\right] = \frac{1}{Z_{3,s}} \int_1^{s/3} \int_{s_3}^{(s-s_3)/2} \frac{(s - s_2 - s_3)^{-1/4} - s^{-1/4}}{(s - s_2 - s_3)^{3/2} s_2^{3/2} s_3^{3/2}} ds_2 ds_3.$$

Two changes of variable help to understand the structure of this rather complicated integral. First, we rescale to remove the dependence of the independent variables on $s$ by setting $s_i = sx_i$. This pushes the $s$-dependence into only a single limit in one of the integrals and a power of $s$ appears as a prefactor. The expression above becomes

$$\frac{1}{Z_{3,s}} s^{-11/4} \int_{1/s}^{1/3} \int_{x_3}^{(1-x_3)/2} \frac{(1 - x_2 - x_3)^{-1/4} - 1}{(1 - x_2 - x_3)^{3/2} x_2^{3/2} x_3^{3/2}} dx_2 dx_3. \tag{8}$$

Second, we notice that

$$(1 - x_3 - x_2)^{-1/4} - 1 = \left[(1 - x_3 - x_2)^{-1/4} - (1 - x_2)^{-1/4}\right] + \left[(1 - x_2)^{-1/4} - 1\right],$$

which leads us to make a further substitution which changes the upper limit of the inner integral to a constant, and 'factorizes' the integrand into parts that depend on the variables separately. Namely, we introduce new variables $y_2$ and $y_3$ defined in terms of $x_2, x_3$ by $x_2 = (1-x_3)y_2$ and $x_3 = y_3$. Hence

8

also $dx_2 = (1 - x_3)dy_2$, and $dx_3 = dy_3$. We also deduce the relation $(1 - x_2 - x_3) = (1 - y_3)(1 - y_2)$. Therefore we can write the double integral in (8) (ignoring for the moment the factor $s^{-11/4}/Z_{3,s}$) as a sum of two terms

$$\underbrace{\int_{\frac{1}{s}}^{\frac{1}{3}} \frac{1}{(1 - y_3)^{\frac{9}{4}} y_3^{\frac{3}{2}}} \int_{\frac{y_3}{(1-y_3)}}^{\frac{1}{2}} \frac{(1 - y_2)^{-\frac{1}{4}} - 1}{(1 - y_2)^{\frac{3}{2}} y_2^{\frac{3}{2}}} dy_2 dy_3}_{I_1} + \underbrace{\int_{\frac{1}{s}}^{\frac{1}{3}} \frac{(1 - y_3)^{\frac{-1}{4}} - 1}{(1 - y_3)^2 y_3^{\frac{3}{2}}} \int_{\frac{y_3}{(1-y_3)}}^{\frac{1}{2}} \frac{1}{(1 - y_2)^{\frac{3}{2}} y_2^{\frac{3}{2}}} dy_2 dy_3}_{I_2}$$

(9)

$I_1$ turns out to be leading order contribution at large $s$: the main contribution comes from the region where $y_3$ and $y_2$ are small. The inner integral

$$\int_{\frac{y_3}{(1-y_3)}}^{\frac{1}{2}} \frac{(1 - y_2)^{\frac{-1}{4}} - 1}{(1 - y_2)^{\frac{3}{2}} \tilde{y}_2^{\frac{3}{2}}} dy_2$$

approaches a finite value as $y_3 \to 0$, and, since we are computing just the leading order term, we therefore investigate replacing the lower limit $y_3/(1 - y_3)$ by zero. The exact value of the integral in the limit $y_3 \to 0$ can be expressed in terms of hypergeometric functions

$$a(\gamma = 4) := \int_0^{\frac{1}{2}} \frac{(1 - y_2)^{\frac{-1}{4}} - 1}{(1 - y_2)^{\frac{3}{2}} y_2^{\frac{3}{2}}} dy_2 = 2\sqrt{2} \left[ {}_2F_1 \left( \frac{3}{2}, -\frac{1}{2}; \frac{1}{2}; \frac{1}{2} \right) - {}_2F_1 \left( \frac{7}{4}, -\frac{1}{2}; \frac{1}{2}; \frac{1}{2} \right) \right]$$

$$\approx 0.59202228363...$$

Further, we note that the error incurred in replacing $\frac{y_3}{1-y_3}$ by 0 is

$$-\int_0^{\frac{y_3}{1-y_3}} \frac{(1 - y_2)^{-1/4} - 1}{(1 - y_2)^{\frac{3}{2}} y_2^{\frac{3}{2}}} dy_2 = -\int_0^{y_3} \frac{1}{4} \frac{1}{y_2^{\frac{1}{2}}} dy_2 + O(y_3^{3/2}) = -\frac{1}{2} y_3^{1/2} + O(y_3^{3/2})$$

for small $y_3$. Now we evaluate the outer integral in $I_1$, which yields

$$\int_{\frac{1}{s}}^{\frac{1}{3}} \frac{a - \frac{1}{2} y_3^{1/2} + O(y_3^{3/2})}{(1 - y_3)^{\frac{9}{4}} y_3^{\frac{3}{2}}} dy_3 = a \, 2\sqrt{s} - \frac{1}{2} \log s + O(1).$$

Therefore, $I_1 = 2a\sqrt{s} - \frac{1}{2} \log(s) + O(1)$, as $s \to \infty$.

Now we evaluate $I_2$ from equation (9). We begin, as in the case of $I_1$, by determining the leading-order behaviour of the inner integral. We find find that

$$\int_{\frac{y_3}{(1-y_3)}}^{\frac{1}{2}} \frac{1}{(1 - y_2)^{\frac{3}{2}} y_2^{\frac{3}{2}}} dy_2 \sim 2y_3^{-1/2} + O(1) \quad \text{as} \quad y_3 \to 0.$$

Substituting this into the outer integral we find that

$$I_2 = \int_{\frac{1}{s}}^{\frac{1}{3}} \frac{(1 - y_3)^{\frac{-1}{4}} - 1}{(1 - y_3)^2 y_3^{\frac{3}{2}}} \left[ \frac{2}{y_3^{1/2}} + O(1) \right] dy_3 = 2 \int_{\frac{1}{s}}^{\frac{1}{3}} \frac{(1 - y_3)^{\frac{-1}{4}} - 1}{(1 - y_3)^2 y_3^{\frac{4}{2}}} dy_3 + O(1)$$

$$= \int_{\frac{1}{s}}^{\frac{1}{3}} \frac{\frac{1}{4} y_3 + O(y_3^2)}{(1 - y_3)^2 y_3^2} dy_3 + O(1)$$

$$= \frac{1}{2} \log s + O(1).$$

9

Combining $I_1$ and $I_2$ we deduce that the asymptotic behaviour of equation (9) is

$$\int_{1/s}^{1/3} \int_{x_3}^{(1-x_3)/2} \frac{(1-x_2-x_3)^{-1/4}-1}{(1-x_2-x_3)^{3/2} x_2^{3/2} x_3^{3/2}} dx_2 dx_3 = 2a\sqrt{s} - \frac{1}{2}\log s + \frac{1}{2}\log s + O(1) \tag{10}$$

$$= 2a\sqrt{s} + O(1).$$

It is interesting to note that the $\log s$ contributions from $I_1$ and $I_2$ exactly cancel. Referring back to equation (8), we now need to reincorporate the factor $s^{-11/4}/Z_{3,s}$. The asymptotic behaviour of the normalising constant $Z_{3,s}$ can be determined using the same changes of variables as used above. We obtain

$$Z_{3,s} = \int_1^{\frac{s}{3}} \int_{s_3}^{\frac{(s-s_3)}{2}} \frac{1}{(s-s_2-s_3)^{\frac{3}{2}} s_2^{\frac{3}{2}} s_3^{\frac{3}{2}}} ds_2 ds_3 = 2s^{-\frac{3}{2}} + O(s^{-2}).$$

Therefore $s^{-11/4}/Z_{3,s} = 2s^{-\frac{5}{4}} + O(s^{-\frac{7}{4}})$ and

$$\mathbf{E}\left[R_1 - s^{-1/4} \middle| N=3,\ S_1+S_2+S_3 = s\right] = a\,s^{-\frac{3}{4}} + O(s^{-\frac{5}{4}}), \quad \text{as } s \to \infty,$$

which gives the asymptotic form of the expected error in the naive heuristic in the case $k=3$, $\gamma = 4$.

## 2.3 Computations for $k \geq 2$ and $\gamma > 2$

In this subsection we essentially repeat the steps set out in the previous subsection but for general values of $k \geq 2$ and $\gamma > 2$. The details become quite intricate and some are deferred to the Appendix, but the structure of the argument remains as before.

Consider, as before, a disk of radius $\rho$, where $0 < \rho < \infty$ and with the number of points distributed as $\mathsf{Poisson}(\lambda\pi\rho^2)$. The probability density in the case in which there are $k$ points at radii $r_1, \ldots, r_k$ in the disk is given by

$$f_{R_1,\ldots,R_k,N=k}(r_1,\ldots,r_k) = (2\lambda\pi)^k r_1 \cdots r_k e^{-\lambda\pi\rho^2} = (2\lambda\pi)^k e^{-\lambda\pi\rho^2} \prod_{i=1}^k r_i. \tag{11}$$

We now write (11) in terms of signal strengths $s_1, \ldots, s_k$ received at the origin, using $r_i = s_i^{-\frac{1}{\gamma}}$. Hence

$$f_{S_1,\ldots,S_k,N=k}(s_1,\ldots,s_k) = (2\lambda\pi)^k e^{-\lambda\pi\rho^2} \prod_{i=1}^k \frac{1}{\gamma} s_i^{-\frac{\gamma+2}{\gamma}}. \tag{12}$$

The variable $s_1$ can be expressed as $s_1 = s - s_2 - s_3 - \cdots - s_k$, so that (12) can be written as

$$f_{S_2,\ldots,S_k \mid N=k,S'=s}(s_2,\ldots,s_k \mid s) = \frac{1}{Z_{k,s}}(s-s_2-\cdots-s_k)^{-\frac{\gamma+2}{\gamma}} \prod_{i=2}^k s_i^{-\frac{\gamma+2}{\gamma}}, \tag{13}$$

where the variables are ordered, and constrained through the requirement that the points all lie in the disk of radius $\rho$, so that $s - s_2 - \cdots - s_k > s_2 > \cdots > s_k > \rho^{-\gamma}$. The normalisation term in (13) now formally depends on four parameters: $k$, $s$, $\gamma$ and $\rho$ but we will tend to suppress the dependence on the final two arguments for clarity:

$$Z_{k,s} \equiv Z_{k,s,\gamma,\rho} = \int_{\rho^{-\gamma}}^{\frac{s}{k}} ds_k \int_{s_k}^{\frac{s-s_k}{k-1}} ds_{k-1} \cdots \int_{s_3}^{\frac{s-s_3-\cdots-s_k}{2}} ds_2\, (s-s_2-\cdots-s_k)^{-\frac{\gamma+2}{\gamma}} s_2^{-\frac{\gamma+2}{\gamma}} \cdots s_k^{-\frac{\gamma+2}{\gamma}}. \tag{14}$$

10

Therefore the expected error $R_1 - s^{-1/\gamma}$ can be written as a set of $k-1$ nested integrals

$$\mathbf{E}\left[R_1 - s^{-\frac{1}{\gamma}} \,\middle|\, N = k, \sum_{i=1}^{k} S_i = s\right] = \frac{1}{Z_{k,s}} \int_{\rho^{-\gamma}}^{\frac{s}{k}} ds_k \cdots \int_{s_3}^{\frac{s - s_3 - \cdots - s_k}{2}} ds_2 \, \frac{\left(s - s_2 - \cdots - s_k\right)^{-\frac{1}{\gamma}} - s^{-\frac{1}{\gamma}}}{\left(s - s_2 - \cdots - s_k\right)^{\frac{\gamma+2}{\gamma}} s_2^{\frac{\gamma+2}{\gamma}} \cdots s_k^{\frac{\gamma+2}{\gamma}}}.$$
$$(15)$$

We now proceed to compute the leading-order asymptotic terms in (15) and (14). We do this in two separate subsections below, starting with (14).

### 2.3.1  Equation (14): evaluating $Z_{k,s}$.

To evaluate (14) we use the same procedure as was illustrated in section 2.2. First we scale out the dependence on $s$ by changing variables from $s_2, \ldots s_k$ to $x_2, \ldots, x_k$ defined by setting $s_i = s x_i$. This gives

$$Z_{k,s} = s^{-\frac{2k}{\gamma}-1} \int_{\rho^{-\gamma}/s}^{\frac{1}{k}} dx_k \int_{x_k}^{\frac{1-x_k}{k-1}} dx_{k-1} \cdots \int_{x_3}^{\frac{1-x_3-\cdots-x_k}{2}} dx_2 \left(1 - x_2 - \cdots - x_k\right)^{-\frac{\gamma+2}{\gamma}} x_2^{-\frac{\gamma+2}{\gamma}} \cdots x_k^{-\frac{\gamma+2}{\gamma}}.$$
$$(16)$$

Second, we then make a further change of variables from $x_2, \ldots, x_k$ to $y_2, \ldots, y_k$ which generalises the one used to achieve equation (9), and that we will now define.

**Definition 1.** *We define the variable $y_i$ for $2 \leq i \leq k$, by*

$$y_i = x_i \left(1 - x_{i+1} - \cdots - x_k\right)^{-1}.$$
$$(17)$$

From the above definition the following lemma follows easily.

**Lemma 1.** *For $x_i$ and $y_i$, where $2 \leq i \leq k$, we have*

$$\left(1 - \sum_{m=i}^{k} x_m\right) = \prod_{m=i}^{k} \left(1 - y_m\right).$$
$$(18)$$

Using these substitutions we find that (16) can be written as

$$Z_{k,s} = s^{-\frac{2k}{\gamma}-1} \int_{\frac{1}{s\rho^\gamma}}^{\frac{1}{k}} dy_k \, y_k^{-\frac{(\gamma+2)}{\gamma}} \left(1 - y_k\right)^{\frac{(2-2k-\gamma)}{\gamma}} \int_{\frac{y_k}{1-y_k}}^{\frac{1}{k-1}} dy_{k-1} \, y_{k-1}^{-\frac{(\gamma+2)}{\gamma}} \left(1 - y_{k-1}\right)^{\frac{(2-2(k-1)-\gamma)}{\gamma}} \cdots$$

$$\cdots \int_{\frac{y_3}{1-y_3}}^{\frac{1}{2}} dy_2 \, y_2^{-\frac{(\gamma+2)}{\gamma}} \left(1 - y_2\right)^{\frac{(2-2(2)-\gamma)}{\gamma}}.$$
$$(19)$$

By defining an iterative sequence $J_k$ we can express (19) more concisely. We define $J_k$ as follows.

**Definition 2** (The sequence of nested integrals $J_k$)**.** *We set:*

$$J_2 \quad := \quad 1$$
$$(20)$$

*and for $3 \leq l \leq k$ we define*

$$J_l \quad := \quad \int_{\frac{y_l}{1-y_l}}^{\frac{1}{l-1}} y_{l-1}^{-\frac{(\gamma+2)}{\gamma}} \left(1 - y_{l-1}\right)^{\frac{(2-2(l-1)-\gamma)}{\gamma}} J_{l-1} \, dy_{l-1}.$$
$$(21)$$

Note that $J_l$ is a function of $y_l$ only. In terms of these nested integrals, we can express the normalisation function as

$$Z_{k,s} = s^{-\frac{(2k+\gamma)}{\gamma}} \int_{\frac{1}{s\rho^\gamma}}^{\frac{1}{k}} y_k^{-\frac{(\gamma+2)}{\gamma}} (1-y_k)^{\frac{(2-2k-\gamma)}{\gamma}} J_k \, dy_k \tag{22}$$

By using (21) to successively investigate the asymptotic behaviour of each $J_k$ we find that the leading order term in the normalisation function is

$$Z_{k,s} = \left(\frac{\gamma}{2}\right)^{(k-1)} \frac{1}{(k-1)!} \rho^{2(k-1)} s^{-\frac{(\gamma+2)}{\gamma}} + O\left(s^{-\frac{(\gamma+4)}{\gamma}}\right). \tag{23}$$

Therefore asymptotically we find, for $k \geq 3$, $\gamma > 2$ and $0 < \rho < \infty$, that

$$Z_{k,s} \equiv Z_{k,s,\gamma,\rho} \sim \left(\frac{\gamma}{2}\right)^{k-1} \frac{1}{(k-1)!} \rho^{2(k-1)} s^{-\frac{(\gamma+2)}{\gamma}} \qquad \text{as } s \to \infty. \tag{24}$$

### 2.3.2 Equation (15): evaluating the integral.

We now turn to the multiple integral $W_{k,s}$ in (15)

$$W_{k,s} := \int_{\rho^{-\gamma}}^{\frac{s}{k}} \cdots \int_{s_3}^{\frac{s-s_3}{s}} \frac{(s-s_2-\ldots-s_k)^{-\frac{1}{\gamma}} - s^{-\frac{1}{\gamma}}}{(s-s_2-\ldots-s_k)^{\frac{\gamma+2}{\gamma}} s_2^{\frac{\gamma+2}{\gamma}} \ldots s_k^{\frac{\gamma+2}{\gamma}}} ds_2 \ldots ds_k. \tag{25}$$

Again, we make the changes of variables $s_i = sx_i$ for $i = 2, \ldots, k$ and then from $x_2, \ldots, x_k$ to $y_2, \ldots y_k$ as defined in (17), leading to the relation (18). From this we find that the numerator of (25) can be expressed as

$$(s-s_2-\ldots-s_k)^{-\frac{1}{\gamma}} - s^{-\frac{1}{\gamma}} = s^{-\frac{1}{\gamma}} \sum_{j=2}^{k} \left( \left[ (1-y_j)^{-\frac{1}{\gamma}} - 1 \right] \prod_{i=j+1}^{k} (1-y_i)^{-\frac{1}{\gamma}} \right). \tag{26}$$

By noting that the denominator of (25) is the same as in the normalising constant expressed in (14) we know that, following the above substitutions, it will contain the same factors as in (19).

We now define another iterative sequence of nested integrals $Q_k^{(j)}$, where $j$ is the variable summed over in (26).

**Definition 3** (The sequence of nested integrals $Q_k^{(j)}$). *Fix $k \geq 3$, then define the quantities $Q_l^{(j)}$, for $1 \leq l \leq k$ and $2 \leq j \leq k$, as follows:*

1. *For all $2 \leq j \leq k$, set*

$$Q_1^{(j)} := 1.$$

2. *For $2 \leq l \leq j-1$, we define*

$$Q_l^{(j)} := \int_{\frac{y_{l+1}}{1-y_{l+1}}}^{\frac{1}{l}} y_l^{-\frac{(\gamma+2)}{\gamma}} (1-y_l)^{\frac{2-2l-\gamma}{\gamma}} Q_{l-1}^{(j)} \, dy_l.$$

3. *For $2 \leq l = j \leq k$, we define*

$$Q_l^{(j)} := \int_{\frac{y_{l+1}}{1-y_{l+1}}}^{\frac{1}{l}} y_l^{-\frac{(\gamma+2)}{\gamma}} (1-y_l)^{\frac{2-2l-\gamma}{\gamma}} \left[ (1-y_l)^{-\frac{1}{\gamma}} - 1 \right] Q_{l-1}^{(j)} \, dy_l.$$

4. For $j + 1 \le l \le k$, we define

$$Q_l^{(j)} := \int_{\frac{y_{l+1}}{1-y_{l+1}}}^{\frac{1}{l}} y_l^{-\frac{(\gamma+2)}{\gamma}} (1 - y_l)^{\frac{1-2l-\gamma}{\gamma}} Q_{l-1}^{(j)} \, dy_l.$$

Note that we define the lower limit of the outermost integral in $Q_k^{(j)}$ separately, setting $\frac{y_{k+1}}{1-y_{k+1}} := \frac{1}{s\rho^\gamma}$.

Using the iterative sequence $Q_k^{(j)}$, we can write expression (25) concisely as

$$W_{k,s} = s^{-\frac{(2k+\gamma+1)}{\gamma}} \sum_{j=2}^{k} Q_k^{(j)} \tag{27}$$

and therefore equation (15) can be expressed as

$$\mathbf{E}\left[R_1 - s^{-1/\gamma} \,\middle|\, \sum_{i=1}^{k} S_i = s\right] = \frac{1}{Z_{k,s}} \left( s^{-\frac{(2k+\gamma+1)}{\gamma}} \sum_{j=2}^{k} Q_k^{(j)} \right). \tag{28}$$

It remains to find the leading-order behaviour of $\sum_{j=2}^{k} Q_k^{(j)}$. The details of this become quite algebraically intensive and are given in Appendix A. It turns out that there are a number of different cases to consider depending on the value of $\gamma$. To summarise, the work in the Appendix demonstrates that for all $\gamma > 2$

$$\sum_{j=2}^{k} Q_k^{(j)} = a(\gamma) \frac{\gamma^{(k-2)}}{2^{(k-2)}(k-2)!} y_{k+1}^{\frac{-2(k-2)}{\gamma}} + O\left( y_{k+1}^{\frac{-2(k-2)}{\gamma}+\varepsilon} \right) \tag{29}$$

where $a(\gamma)$ is as given in (3), and $\varepsilon = \min\left\{\frac{\gamma-2}{\gamma}, \frac{2}{\gamma}\right\}$.

By combining this with (28) and substituting $y_{k+1} = \frac{1}{s\rho^\gamma}$ we find that

$$\mathbf{E}\left[R_1 - s^{-\frac{1}{\gamma}} \,\middle|\, N = k, \sum_{i=1}^{k} S_i = s\right] = \frac{1}{Z_{k,s}} \left( a(\gamma) s^{-\frac{(\gamma+5)}{\gamma}} \left(\frac{\gamma}{2}\right)^{(k-2)} \frac{1}{(k-2)!} \rho^{2(k-2)} + O\left( s^{-\frac{\gamma+5}{\gamma}-\varepsilon} \right) \right) \tag{30}$$

Therefore, asymptotically for large $s$,

$$\mathbf{E}\left[R_1 - s^{-1/\gamma} \,\middle|\, N = k, S' = s\right] \sim \frac{1}{Z_{k,s}} a(\gamma) \left(\frac{\gamma}{2}\right)^{k-2} \frac{1}{(k-2)!} \rho^{2(k-2)} s^{-1-5/\gamma}$$

$$\sim \frac{a(\gamma)\, 2\, (k-1)}{\gamma} \rho^{-2} s^{-3/\gamma}, \quad \text{as } s \to \infty.$$

More detailed error estimates for this expression could be computed by taking into account additional lower order terms.

## 2.4 Summing over the number of transmitters $k \geq 1$

Having computed the expectation conditioned on a fixed number of transmitters $k$, we now sum the estimates of section 2.3 over $k \geq 1$ to derive the expectation for the total signal strength. To do this rigorously, we would need to take into account $k$-dependence in the constants in our error terms. We have not fully investigated this and leave a completely rigorous consideration to be the subject of future work. Comparing our theoretical results against numerical simulations indicates that the asymptotic structure of our results holds, and is quantitatively useful over a wide range of signal strengths, so that this point does not, in practice, appear to be a limitation.

We first compute the probability density of the total signal strength

$$
\begin{aligned}
f_{S'}(s) &= \sum_{k=1}^{\infty} e^{-\lambda\pi\rho^2} \left(\frac{2\lambda\pi}{\gamma}\right)^k Z_{k,s,\gamma,\rho} \\
&\sim e^{-\lambda\pi\rho^2} \sum_{k=1}^{\infty} \left[ \left(\frac{2\lambda\pi}{\gamma}\right)^k \left(\frac{\gamma}{2}\right)^{k-1} \frac{1}{(k-1)!} \rho^{2(k-1)} s^{-1-2/\gamma} \right] \\
&= \frac{2\lambda\pi}{\gamma} s^{-1-2/\gamma} e^{-\lambda\pi\rho^2} \sum_{k=1}^{\infty} \frac{(\lambda\pi\rho^2)^{k-1}}{(k-1)!} \\
&= \frac{2\lambda\pi}{\gamma} s^{-1-2/\gamma}, \quad \text{as } s \to \infty.
\end{aligned}
$$

With this estimate at hand, we can compute the probability of having $k$ transmitters, conditional on the signal strength being large:

$$
\begin{aligned}
\mathbf{P}[N = k \,|\, S' = s] &= \frac{1}{f_{S'}(s)} e^{-\lambda\pi\rho^2} \left(\frac{2\lambda\pi}{\gamma}\right)^k Z_{k,s,\gamma,\rho} \\
&\sim \frac{\gamma}{2\lambda\pi s^{-1-2/\gamma}} \left( \frac{2\lambda\pi}{\gamma} e^{-\lambda\pi\rho^2} \frac{(\lambda\pi\rho^2)^{k-1}}{(k-1)!} s^{-1-2/\gamma} \right) \\
&= e^{-\lambda\pi\rho^2} \frac{(\lambda\pi\rho^2)^{k-1}}{(k-1)!}, \quad \text{as } s \to \infty, \text{ for } k = 1, 2, \ldots.
\end{aligned}
$$

We observe that this discrete distribution on $k$ is Poisson distributed. That is, conditionally on a large signal, the number $k-1$ of *extra transmitters* (in addition to the nearest one), is asymptotically Poisson$(\lambda\pi\rho^2)$. This yields

$$
\begin{aligned}
\mathbf{E}\left[R_1 - s^{-1/\gamma} \,\Big|\, S' = s\right] &\sim \sum_{k=1}^{\infty} e^{-\lambda\pi\rho^2} \frac{(\lambda\pi\rho^2)^{k-1}}{(k-1)!} \frac{2(k-1)\,a(\gamma)\,\rho^{-2}}{\gamma} s^{-3/\gamma} \\
&\sim \frac{2\lambda\pi}{\gamma} a(\gamma) s^{-3/\gamma}, \quad \text{as } s \to \infty, \text{ independent of the value of } \rho.
\end{aligned}
$$
(31)

Therefore we conclude that

$$
\mathbf{E}\left[R_1 \,\Big|\, S' = s\right] = s^{-1/\gamma} + \frac{2\lambda\pi}{\gamma} a(\gamma) s^{-3/\gamma} + o(s^{-3/\gamma}).
\tag{32}
$$

## 3 Comparison with numerical simulations

In this section we use numerical simulations to assess and compare the performance of the asymptotic approximation (32) with the heuristic $R_1 = s^{-1/\gamma}$. To do this we begin by simulating the distribution

of $R_1$ for a given value of $s$, using rejection sampling. For simulation with a target value $S = s$, a set of distances $R_1 < R_2 < \cdots < R_{100}$ were simulated, and the sample was rejected if $\sum_{k=1}^{100} R_k^{-\gamma} \notin [0.98s, 1.02s]$. Simulation results were not sensitive to any further increase in the number of distances considered beyond 100. That such a choice is justified is also borne out by our theoretical calculations which show that an $O(1)$ number of transmitters determine the asymptotics. For the simulations where $\gamma = 4$ and $6$, $2 \times 10^6$ samples were used and for the simulation when $\gamma = 3$, $5 \times 10^6$ samples were used. The two choices regarding accuracy and sample size provide an acceptable trade-off between simplicity of simulation and accuracy, the simulations produce values close to our theoretical values.

Figures 2 and 3 show the distribution of $R_1$ for $\gamma = 4$, in the two cases $s = 50$ and $s = 1000$, respectively. It is clear that the overall shape of the distribution also changes significantly with $s$; further analysis of the distribution is described in Jarai (2019).

While transmitter locations are distributed according to a Poisson point process in the plane, we are only interested in the distances of these transmitters to the origin, not their planar location. The Mapping Theorem can be used to efficiently generate sets of correctly distributed distances. Efficiency is required since the rejection sampling method often requires a very large number of samples to be generated in order to achieve acceptable statistical accuracy.

The Mapping Theorem (Last & Penrose, 2017, theorem 5.1 in chapter 5) allows us to generate realisation of the random variables $R_1 < R_2 < \cdots < R_{100}$ in a more efficient way that simulating the Poisson point process directly. We do this as follows: let $\lambda$ be the intensity of the Poisson point process and then generate 100 i.i.d. random variables distributed $\mathsf{Exp}(\lambda\pi)$. These exponential variables are then mapped to the required distances by taking the square root of their cumulative sum. To ensure independence, a new set of transmitter distances was generated for each sample.
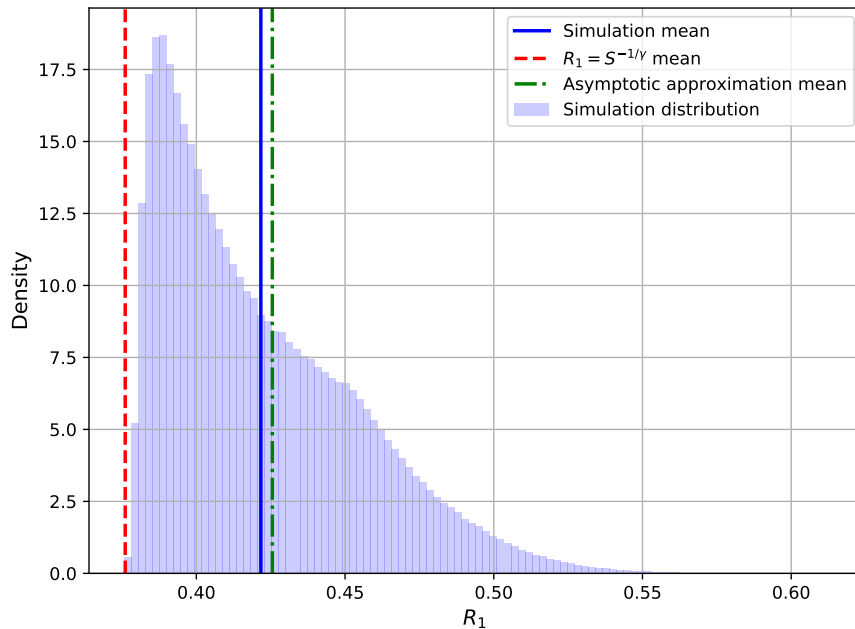


Figure 2: Distribution of the distance $R_1$ from the origin to the nearest transmitter for the case $s = 50$ ('small total signal strength') and path loss $\gamma = 4$. A total of $2 \times 10^6$ sample values of $S$ were used. The simulation mean (solid blue line) is close to the asymptotic approximation (green dash-dotted line) while the naive heuristic $s^{-1/\gamma}$ significantly underestimates the distribution mean.

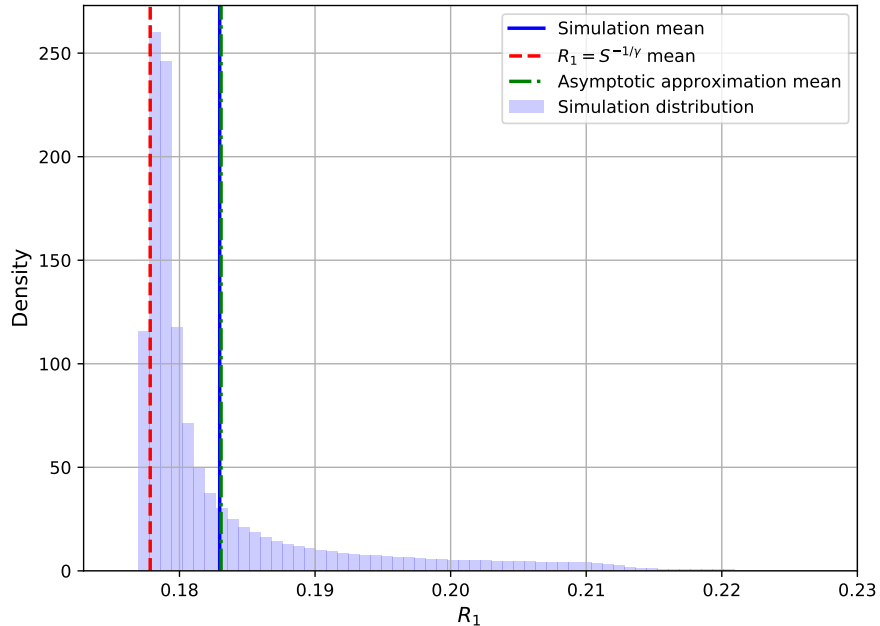Figure 4 compares the accuracy of the naive heuristic and the asymptotic approximation for

Figure 3: Distribution of the distance $R_1$ from the origin to the nearest transmitter for the case $s = 1000$ ('large total signal strength') and path loss $\gamma = 4$. The simulation mean (solid blue line) is extremely close to the asymptotic approximation, while again the naive heuristic significantly underestimates the mean.

three different values of path loss, $\gamma = 3, 4, 6$, over a range of values of $s$. The values for path loss were chosen to be close to observed real world values and indicate how the accuracy of these approximations varies for values of $\gamma$ higher and lower than $\gamma = 4$. The accuracy of the asymptotic approximation increases as $\gamma$ decreases. This is due to the error being $O(s^{-3/\gamma - \varepsilon})$ as shown previously in section 2. The naive heuristic $R_1 = s^{-1/\gamma}$ has error of order $O(s^{-3/\gamma})$ and therefore for large $s$, the accuracy increases as $\gamma$ decreases. This behaviour can also be seen in Figure 4. We note that for smaller $s$ this is reversed.

| Heuristic | Theory | | Observed |
|---|---|---|---|
| Asymptotic Approximation, $\gamma = 3$ | -5/3 | (-1.67) | -1.581 |
| Asymptotic Approximation, $\gamma = 4$ | -5/4 | (-1.25) | -1.214 |
| Asymptotic Approximation, $\gamma = 6$ | -5/6 | (-0.83) | -0.786 |
| Naive heuristic $r_1 = s^{-1/3}$ | -3/3 | (-1.00) | -1.015 |
| Naive heuristic $r_1 = s^{-1/4}$ | -3/4 | (-0.75) | -0.730 |
| Naive heuristic $r_1 = s^{-1/6}$ | -3/6 | (-0.50) | -0.468 |

Table 1: Comparison of the gradients of the best-fit lines plotted in figure 4 ('Observed') with the theoretical values. In all cases there is excellent agreement between the two.
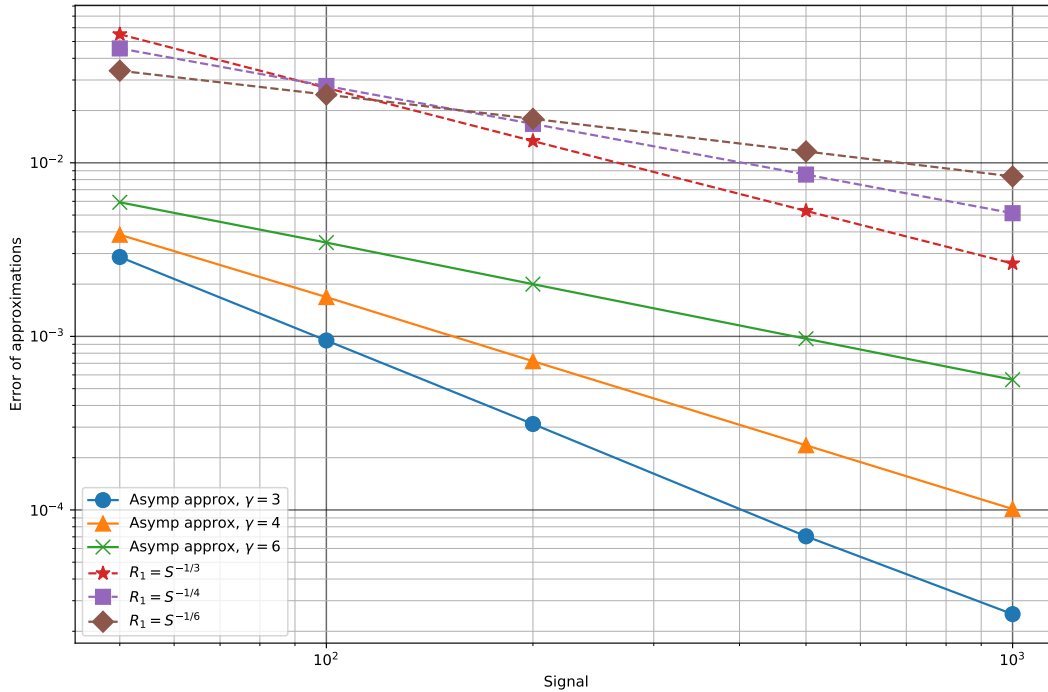
Figure 4: This graph shows on log-log axes the error of the approximations (compared to high-precision numerical simulations) decreasing as total signal strength increases, for different values of $\gamma$. The approximation error is the absolute value (in %) of the difference between the estimate and the actual value from numerics, i.e., error $= \frac{100(\text{theory-numerical})}{\text{numerical}}$. The asymptotic approximation is significantly more accurate than the naive heuristic $r_1 = s^{-1/\gamma}$ over all relevant values of $s$. The gradients of the lines match those expected theoretically from the heuristics and are compared directly in table 1.

# 4 Rayleigh fading

In the Introduction we briefly described the issue of 'fading' as a propagation effect that further reduced signal strengths. In sections 2 and 3 we considered situations without fading; in this section we examine how it might be possible accurately to estimate the distance to the nearest transmitter when the effect of fading is included.

Our first approach, described in subsection 4.1, is to compute a scaling factor that can be used to scale the faded signal to the values it would have taken been had fading not been in effect. The recovered signal can then be used in conjunction with a distance heuristic to estimate the distance to the nearest transmitter. The scaling factor approach can be used for Nakagami-$m$ fading, although we use the Rayleigh fading case, corresponding to $m = 1$, for illustrative purposes. In subsection 4.2 we develop an improved heuristic for finding the expected distance to the nearest transmitter based on observed faded signal at the origin. Both methods are then compared against numerical simulations in subsection 4.3.

## 4.1 The scaling factor approach

We begin by recalling scaling properties of the total signal (Haenggi, 2012, Section 5.1). Let $R_1 < R_2 < \ldots$ be the distances from the origin to a countable collection of transmitters distributed according to a Poisson point process with intensity $\lambda$. The total signal received at the origin without fading is

$$S(\lambda) = \sum_{i=1}^{\infty} R_i(\lambda)^{-\gamma},$$

where our notation emphasizes that the distribution of $S$ depends on $\lambda$. When fading is present, we have instead a total signal

$$T(\lambda) = \sum_{i=1}^{\infty} H_i R_i(\lambda)^{-\gamma},$$

where $H_1, H_2, \ldots$ are independent random variables taking values in $(0, 1]$ describing the Nakagami-$m$ fading. Note that in Haenggi (2012) the total signal is referred to as 'interference' and is denoted by $I(\lambda)$. By calculating Laplace transforms, it can be shown (Haenggi, 2012, Section 5.1.7) that $T(\lambda)$ has the same distribution as $S(\mathbf{E}[H^{2/\gamma}]\lambda)$. It can also be shown (Haenggi, 2012, Corollary 5.4) that for any positive constant $a$, $S(a\lambda)$ has the same distribution as $a^{\gamma/2}S(\lambda)$. It follows from these two facts that

$$T(\lambda) \overset{\mathrm{d}}{=} \mathbf{E}[H^{2/\gamma}]^{\gamma/2}S(\lambda),$$

where $\overset{\mathrm{d}}{=}$ means equal in distribution. Hence $\mathbf{E}[H^{2/\gamma}]^{\gamma/2}$ is a scaling factor of the kind we are looking for.

Nakagami-$m$ fading employs random variables that are $\mathsf{Gamma}(m, 1/m)$ - distributed. The probability density function of the $\mathsf{Gamma}(\alpha, \theta)$ distribution with shape $\alpha > 0$ and scale $\theta > 0$ is given by

$$f(x; \alpha, \theta) = \frac{1}{\Gamma(\alpha)\theta^{\alpha}}x^{\alpha-1}e^{-\frac{x}{\theta}} \quad \text{for } 0 < x < \infty,$$

and therefore

$$\mathbf{E}[H^{2/\gamma}] = \frac{1}{\Gamma(m)(1/m)^m} \int_0^{\infty} h^{\frac{2}{\gamma}+m-1}e^{-mh}\,dh.$$

A simple change of variables shows that

$$\int_0^{\infty} h^{\frac{2}{\gamma}+m-1}e^{-mh}\,dh = (1/m)^{\frac{2}{\gamma}+m}\Gamma(\frac{2}{\gamma}+m)$$

which implies

$$\mathbf{E}[H^{2/\gamma}] = \frac{\Gamma(\frac{2}{\gamma} + m)(1/m)^{\frac{2}{\gamma}}}{\Gamma(m)}.$$

Hence our scaling factor $c(\gamma, m)$ can be defined as

$$c(\gamma, m) := \mathbf{E}\left[H^{2/\gamma}\right]^{\gamma/2} = \left(\frac{\Gamma(\frac{2}{\gamma} + m)}{\Gamma(m)}\right)^{\gamma/2} \frac{1}{m}. \tag{33}$$

Based on this scaling result, the naive heuristic can be adjusted to yield:

$$R_1(\lambda) \approx S(\lambda)^{-1/\gamma} \stackrel{\mathrm{d}}{=} c(\gamma, m)^{1/\gamma} T(\lambda)^{-1/\gamma}. \tag{34}$$

We refer to this heuristic as '$R_1 = T^{-1/\gamma}$ with scaling'. The asymptotic approximation (32) combined with the scaling factor gives

$$\mathbf{E}\left[R_1 \middle| T = t\right] \approx t^{-1/\gamma} c(\gamma, m)^{1/\gamma} + \frac{2\lambda\pi}{\gamma} a(\gamma) t^{-3/\gamma} c(\gamma, m)^{3/\gamma}. \tag{35}$$

We refer to this heuristic as the 'asymptotic heuristic with scaling'.

## 4.2 Distance estimation with Rayleigh fading

The scaling factor approach of the previous subsection can be improved, for the case of Rayleigh fading in which the fading effect is strongest, by computing the distribution of the nearest transmitter $R_1$, not just its mean.

The effect of Rayleigh fading is described by the random variable $H_1$ distributed as $\mathsf{Exp}(1)$, with probability density function

$$f_{H_1}(h_1) = e^{-h_1} \quad \text{where } h_1 > 0.$$

In order to simplify computations, we assume that there is a single transmitter in the disk of radius $\rho = 1/\sqrt{\lambda\pi}$ (for this choice of radius the expected number of transmitters in the disk is 1). Let $\tilde{S}_1$ be the signal contributed by this single transmitter, so that by setting $k = 1$ in (12) we obtain

$$f_{\tilde{S}_1}(s_1) = 2\lambda\pi e^{-\lambda\pi\rho^2} \frac{1}{\gamma} s_1^{-\frac{\gamma+2}{\gamma}} = \frac{2}{\gamma\rho^2} e^{-1} s_1^{-\frac{\gamma+2}{\gamma}}, \quad \rho^{-\gamma} < s_1 < \infty. \tag{36}$$

Continuing with this simplifying assumption, we replace $T$ by the random variable

$$\tilde{T}_1 = H_1 \tilde{S}_1.$$

The joint probability density function of $\tilde{S}_1$ and $H_1$, assumed independent, is given by

$$f_{\tilde{S}_1, H_1}(s_1, h_1) = \frac{2}{\gamma\rho^2} s_1^{-\frac{\gamma+2}{\gamma}} e^{-h_1} e^{-1}.$$

Then the joint probability density function of $\tilde{T}_1$ and $H_1$ is

$$f_{\tilde{T}_1, H_1}(t_1, h_1) = \frac{2}{\gamma\rho^2} h_1^{\frac{2}{\gamma}} t_1^{-\frac{(\gamma+2)}{\gamma}} e^{-h_1} e^{-1}, \quad \text{for} \quad 0 < t_1 < \infty, \text{ and } 0 < h_1 < \rho^\gamma t_1.$$

Since

$$\int_0^{\rho^\gamma t_1} h_1^{2/\gamma} e^{-h_1} dh_1 = \gamma_{\text{lower}}\left(\frac{\gamma + 2}{\gamma}, \rho^\gamma t_1\right),$$

19

where $\gamma_{\text{lower}}$ denotes the lower incomplete Gamma-function, the marginal probability density of $\tilde{T}_1$ is given by

$$f_{\tilde{T}_1}(t_1) = \frac{2}{\gamma \rho^2} t_1^{-\frac{(\gamma+2)}{\gamma}} e^{-1} \gamma_{\text{lower}}\left(\frac{\gamma+2}{\gamma}, \rho^\gamma t_1\right), \quad 0 < t_1 < \infty.$$

We use this to find the conditional distribution

$$f_{H_1|\tilde{T}_1=t_1}(h_1) = \frac{f_{\tilde{T}_1,H_1}(t_1,h_1)}{f_{\tilde{T}_1}(t_1)} = \frac{1}{\gamma_{\text{lower}}\left(\frac{\gamma+2}{\gamma}, \rho^\gamma t_1\right)} h_1^{\frac{2}{\gamma}} e^{-h_1}, \quad 0 < h_1 < \rho^\gamma t_1.$$

Since we made the approximation that $T$ is attributed entirely to the nearest transmitter, we have $t_1 = \tilde{S}_1 H_1 = R_1^{-\gamma} H_1$ and therefore $H_1 = t_1 R_1^\gamma$. From this we find

$$f_{R_1|\tilde{T}_1=t_1}(r_1|t_1) = f_{H_1|\tilde{T}_1=t_1}(h_1|t_1)\frac{dh_1}{dr_1} = f_{H_1|\tilde{T}_1=t_1}(h_1|t_1) t_1 \gamma r_1^{\gamma-1},$$

and therefore

$$f_{R_1|\tilde{T}_1=t_1}(r_1) = \left[\frac{\gamma t_1^{\frac{\gamma+2}{\gamma}}}{\gamma_{\text{lower}}\left(\frac{\gamma+2}{\gamma}, \rho^\gamma t_1\right)}\right] \times r_1^{\gamma+1} e^{-t_1 r_1^\gamma}, \quad 0 < r_1 < \rho. \tag{37}$$

Note that this expression for the probability density of $R_1$ still depends on the radius of the disk has on the probability density function, but when $t_1$ is large the value of $\gamma_{\text{lower}}(\cdot, \cdot)$ does not depend as strongly on $\rho$ as it does when $t_1$ is small.

The expected distance to the nearest transmitter, conditional on observed faded signal at the origin, is therefore given from (37) by

$$\mathbf{E}[R_1|\tilde{T}_1 = t_1] = \frac{\Gamma\left(\frac{\gamma+3}{\gamma}\right)}{t_1^{\frac{1}{\gamma}} \gamma_{\text{lower}}\left(\frac{\gamma+2}{\gamma}, \rho^\gamma t_1\right)} \tag{38}$$

## 4.3   Numerical simulations

To check the accuracy of the appromated distribution and mean for the nearest transmitter estimate, derived in subsection 4.2 for the Rayleigh fading case, we use the same rejection sampling strategy as previously described. We simulate Poisson distributed points for transmitters and the corresponding fading variables. If the computed total faded signal $T$ at the origin is within 2% of the target value then the simulation result is kept, otherwise it is rejected. Five values of $T$ were considered: 50, 100, 200, 500 and 1000 and we generated $10^6$ samples for each of the five values of $T$.

The theoretically approximated distribution and expected mean of $R_1$, given in equations (37) and (38) respectively, are compared to the numerical results in Figures 5 and 6, for the lowest and highest of the five values of $T$. They confirm that the theoretical results perform well across a range of values for $T$. Not surprisingly, agreement is better for the large value of $T$, but even for the lowest value considered, Figure 5 indicates that the approximation remains useful.

Figures 7 and 8 summarise the relative accuracy of the three approximations 34, 35 and (38), derived for distance estimation in the presence of Rayleigh fading. The scaling factor used together with the simple heuristic $R = S^{-1/\gamma}$ gives (34) and is referred to as '$R_1 = T^{-1/\gamma}$ with scaling'. The scaling factor used together with the asymptotic heuristic (32) gives (35) which is referred to as 'Asymptotic heuristic with scaling'. Figure 7 illustrates the performance of (35) and (34), compared to the fading approximation (38), when $\gamma = 4$.
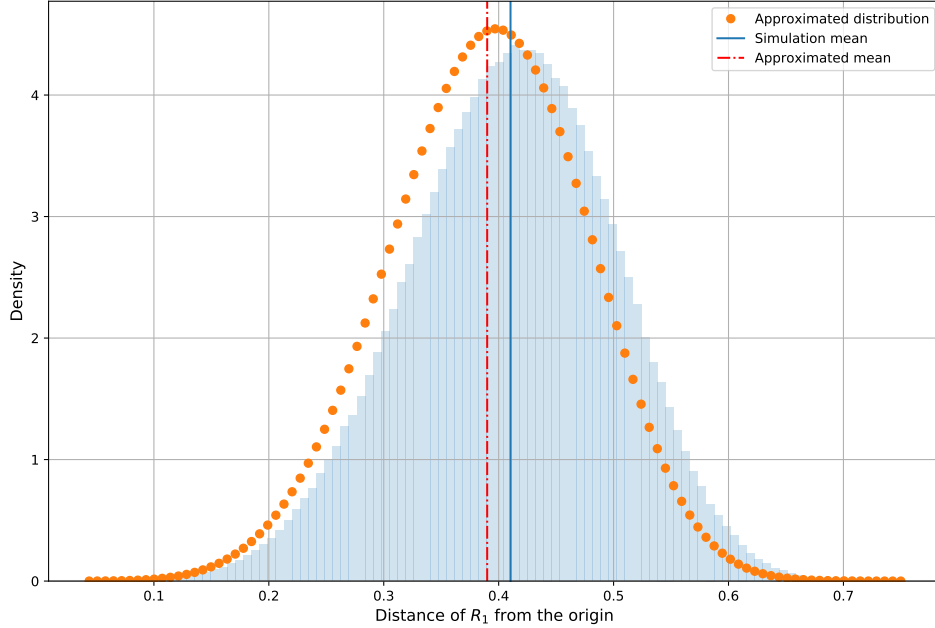
Figure 5: Comparison of theoretical and numerical results for the distribution of $R_1$ for the lowest value $T = 50$, setting $\gamma = 4$ and $\rho = 1$. The (blue) histogram shows the distribution of $R_1$ obtained through numerical simulation, while the (orange) dots indicate the theoretical prediction given by (37), referred to as the 'Approximated distribution'. The overall shape of the theoretical distribution is correct, but it is shifted slightly to the left. The expected mean $R_1$ from equation (38) (red dash-dotted line) is close to the mean obtained from the numerical simulations (blue solid line).

In figure 7 we note that the 'fading approximation' is the most accurate of the three methods, followed by the 'Asymptotic heuristic with scaling'. At all signal strengths the 'fading approximation' underestimates the expected distance $r_1$, whereas the 'Asymptotic heuristic with scaling' appears to provide an overestimate at small signal strengths but is then a slight underestimate at larger signal strengths.

In figure 8 we compare the 'Asymptotic heuristic with scaling' against the 'Fading approximation' for three separate values of $\gamma$: $\gamma = 3, 4, 6$. We see that the 'fading approximation' consistently underestimates $r_1$ whereas the 'Asymptotic heuristic with scaling' again overestimates at sufficiently small signal strengths (probably for all $\gamma > 2$) and then underestimates as $s$ increases. From Figure 8 we conclude that the fading approximation is the most accurate of the three methods, at least in the case with Rayleigh fading.

Figure 9 provides a comparison between the accuracy of the best of the three approximations above, i.e., the 'fading approximation' (38) that attempts to incorporate these propagation effects, and the asymptotic approximation derived in th case of no fading, i.e., (32), in order to assess the relative accuracy of our attempt to extend the distance estimation to the case of Rayleigh fading. We see that the approximation without fading is significantly more accurate, especially for lower values of $\gamma$, which suggests that fading makes estimation of an accurate asymptotic result significantly more complicated.
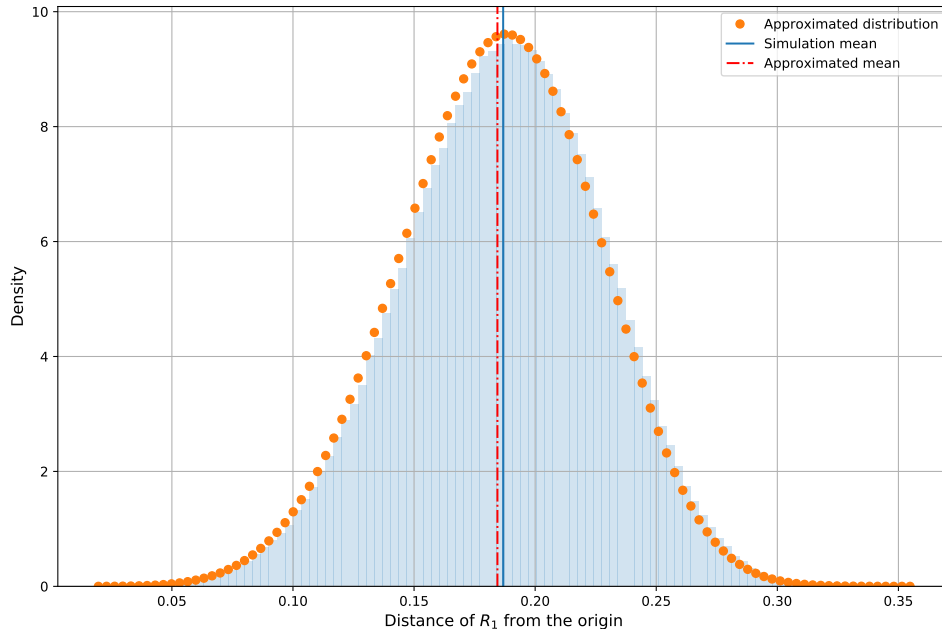
21

Figure 6: Comparison of theoretical and numerical results for the distribution of $R_1$ for the highest value $T = 1000$, setting $\gamma = 4$ and $\rho = 1$. The (blue) histogram shows the distribution of $R_1$ obtained through numerical simulation, while the (orange) dots indicate the theoretical prediction given by (37), referred to as the 'Approximated distribution'. Agreement between theory and numerical simulation is extremely good across the entire range of $R_1$. Consequently, the theoretical mean (read dash-dotted line) and mean obtained through numerical simulations (blue solid line) are extremely close.
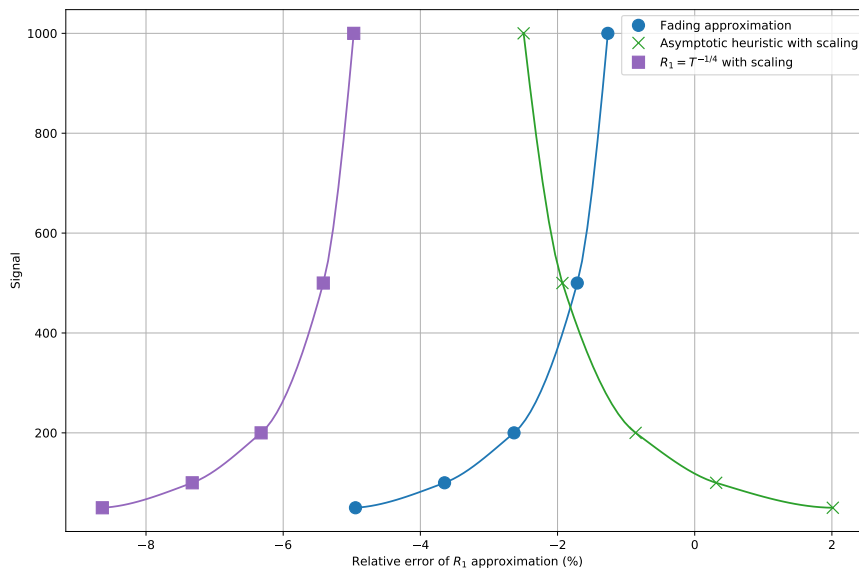


Figure 7: Comparison of the accuracy of the 'fading approximation' (38) with 'that of the 'Asymptotic heuristic with scaling' (35) and '$R_1 = T^{-1/4}$ with scaling' (34) approaches. The path-loss exponent $\gamma = 4$ in all cases.

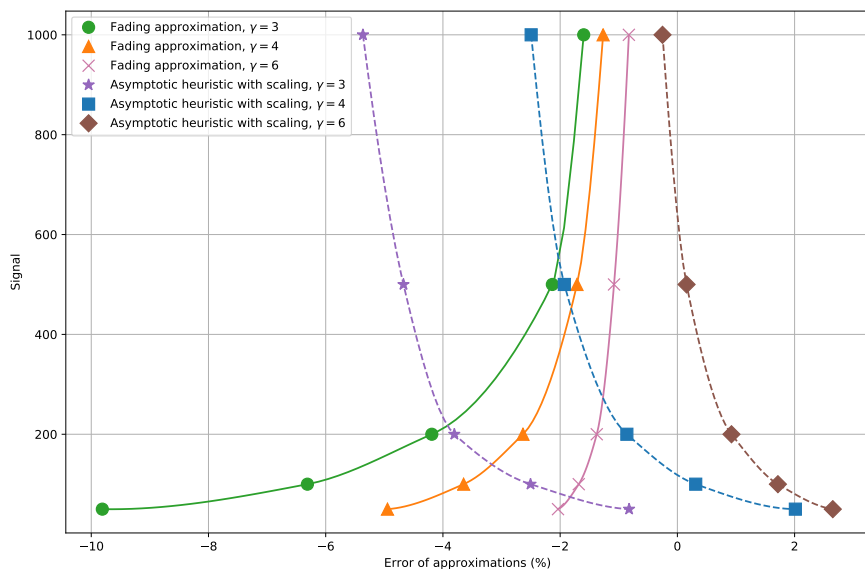Figure 8: Comparing the performance of the fading approximation (38) against the asymptotic heuristic with scaling, for three values of $\gamma$: $\gamma = 3, 4, 6$. Both approximations improve as $\gamma$ increases.
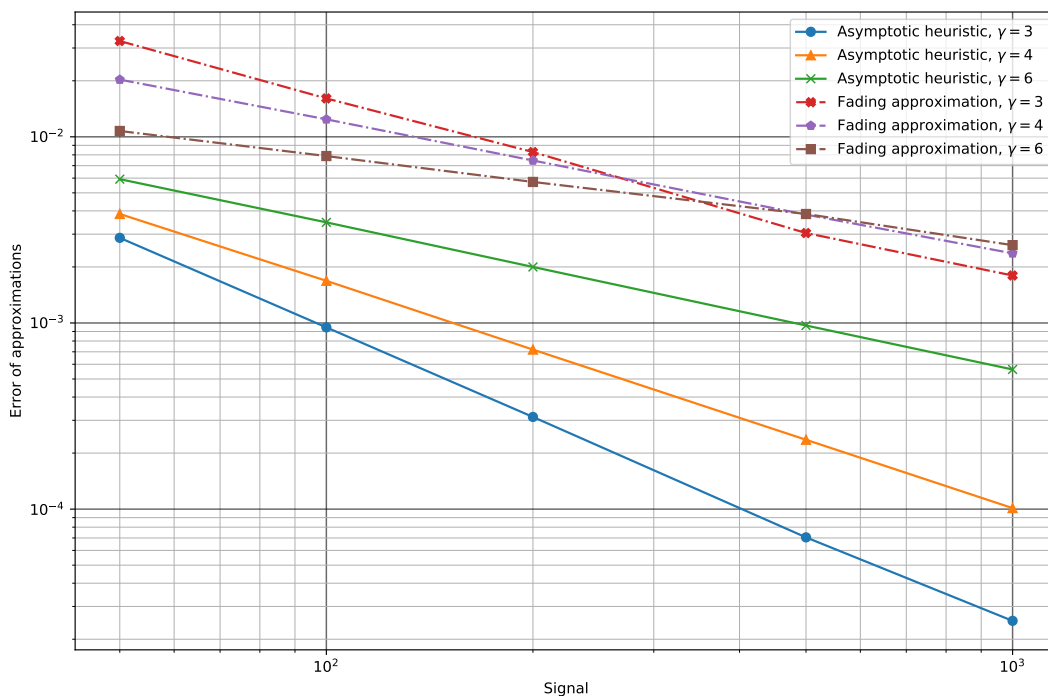


Figure 9: Comparison between approximation errors for distance to nearest transmitter, with and without Rayleigh fading, as a function of signal strength. Results are shown for three values of the path-loss exponent: $\gamma = 3, 4$ and $6$. In the case without fading, the asymptotic heuristic (32) (lower three lines) provides more accurate estimates than the 'fading approximation' (38) does when Rayleigh fading is present.

# 5 Summary and conclusions

In order to operate efficiently, small-cell wireless communications networks increasingly demand 'self-organisation'. This relies on the capability of individual transmitters to gain information about their local network through measurements and data reported by user devices connected to that transmitter. Over the next few years, the rollout and expansion of the 5G network will result in significantly increased densities of small-cell networks. Within these regions of dense coverage in particular, SON technology will help to reduce operating costs and improve user experience. It is highly likely that devices from different manufacturers will need to work collaboratively to optimise the network, but that detailed information on operating characteristics will remain commercially confidential. As a result, individual devices will need to be able to infer properties from network data, such as reported SIRs, alone. Estimating the distance to the nearest neighbour is immediately useful, allowing a transmitter to adjust its power setting to help optimise SIR over the wider network. Therefore the ability of transmitters to estimate, based solely on observations, the distance to the nearest transmitter helps enable distributed self-optimisation. In this paper we have theoretically derived better heuristics than are commonly used in the literature.

In this paper we developed methods for accurately estimating the distance to the nearest neighbour transmitter in such a wireless network. First we ignored propagation effects and considered signal strength to be directly related to separation between transmitter and receiver through a path-loss exponent $\gamma$. We started from the the heuristic that this implies, namely that a measured signal strength $s$ and known path-loss exponent $\gamma$ resulted in an estimate of the distance to the nearest transmitter $r_1$ in the form $r_1 = s^{-1/\gamma}$. This naive approximation can be significantly improved through an asymptotic analysis in the limit of large signal strength, which resulted in (32) which we referred to as the asymptotic approximation. In section 3 the improved accuracy of this heuristic is demonstrated with numerical simulations; even for relatively small values of the observed signal $s$.

In terms of relevance to applications, we note that many studies do indeed analyse high signal power regimes, usually expressed by showing results over a range of SINR (signal to interference-plus-noise) values that spans typically from around $-10$dB to 20dB. More precisely, suppose that we define SINR $= 10 \log_{10}[S/(I + \sigma^2)]$dB where $S$ and $I$ are the signal and interference power, respectively, and $\sigma^2$ is a noise term. Since here we neglect noise and interference, essentially setting $I + \sigma^2$ to unity, we essentially express $S$ as a multiple of interference-plus-noise. Then a signal strength $S = 10^3$ would correspond to SINR $= 30$dB and $S = 10^2$ would correspond to SINR $= 20$dB. We conclude that although our results are derived in the limit of large $S$ they appear to be useful at least down to these values; see for example Figure 4 which indicates errors well below 0.1% even when $S \approx 10$.

Second, we developed in section 4 an improved approximation for the distance to the nearest transmitter in the presence of Rayleigh fading. The inclusion of fading makes the analysis more difficult, and we started our analysis of fading started (in section 4.1) by considering the more general case of Nakagami-$m$ fading and presenting a scaling factor argument to relate the fading case to the non-fading case studied first, in order to make full use of our detailed work on the non-fading case. The most extreme case of Nakagami-$m$ fading is $m = 1$ - the Rayleigh fading case. The case $m = 1$ also turns out to be more tractable analytically and in subsection 4.2 we derived an estimate for the distribution of the distance $R_1$ to the nearest transmitter, conditional on a measured Rayleigh-faded signal $T$. From this distribution we could compute the expected value of $R_1$ conditional on $T$, this expected value (38) is referred to as the 'fading approximation' (to the distance $r_1$). In subsection 4.3 we compared the theoretical results based on the scaling factor and fading approximation arguments to numerical simulations. These indicate that the fading approximation is the most accurate of the three methods discussed for estimating the distance to

the nearest transmitter in cases that include Rayleigh fading.

Overall, our results provide significant improvements over existing naive estimates, yet remain reasonably tractable and fast to compute. There are, naturally, modelling limitations, most obviously that we assume the stochastic geometry of the transmitter network is given by a Poisson point process, and that transmitters are identical - for example they broadcast on the same power settings. However, our general approach of working in the asymptotic limit of large signal strength $s$ is likely to be an approach that applies when these other modelling constraints are relaxed, and results derived in this limit are likely to hold over a wider range of relevant signal strengths.

Of the many directions for future work, two that appear promising are, firstly, to extend these results to cases in which transmitters have different power settings, for example chosen at random with equal probabilities from a discrete set. Although this appears to undermine the central intuition, that large values of received signal correspond to a single nearby transmitter, it seems possible to explore scenarios first in which the power settings have a small range, and therefore this intuition may remain approximately valid.

A second direction for future research is to vary the point process used to define the locations of the transmitters, for example by using an inhomogeneous Poisson point process (perhaps one that is radially symmetric) or a spatially correlated process such as the Mátern or Ginibre processes (Deng et al., 2015; Haenggi, 2017; Kong et al, 2018). Although these are well-known to be less analytically tractable than the homogeneous Poisson point process, the use of the asymptotic limit of large signal strength may allow mathematical progress to be made.

# Funding

# Acknowledgements

# References

Andrews, J., Ganti, R., Haenggi, M., Jindal, N. & Weber, S. (2010) A primer on spatial modeling and analysis in wireless networks. *IEEE communications magazine*, **48**(11), 156–163.

Andrews, J.G., Baccelli, F. & Ganti, R.K. (2011) A tractable approach to coverage and rate in cellular networks. *IEEE Transactions on Communcations*, **59**(11), 3122–3134.

Carle, G., Pahl, M.-O., Raumer, D., Schwaighofer, L., Baumgarten, U. & Söllner, C., editors (2013) *Self-Configuration in LTE Self Organizing Networks*, volume NET-2013-08-1 of *Network Architectures and Services (NET)*, Munich, Germany. Chair for Network Architectures and Services, Department of Computer Science, Technische Universität München.

Cheung, W. C., Quek, T. Q. S. & Kountouris, M. (2012) Throughput Optimization, Spectrum Allocation, and Access Control in Two-Tier Femtocell Networks. *IEEE Journal on Selected Areas in Communications*, **30**(3), 561–574.

Deloitte (2018) 2018 Telecommunications Industry Outlook: A new era of connectivity is on the horizon.
https://www2.deloitte.com/us/en/pages/technology-media-and-telecommunications/articles/telecommunications-industry-outlook.html [Accessed: September 2018].

Deng, N., Zhou, W. & Haenggi, M. (2015) The Ginibre point process as a model for wireless networks with repulsion. *IEEE Transactions on Wireless Communications* **14**(1), 107–121.

Haenggi, M. (2012) *Stochastic Geometry for Wireless Networks*. Cambridge University Press, Cambridge.

Haenggi, M. (2017) User point processes in cellular networks. *IEEE Wireless Communications Letters*, **6**(2), 258–261.

Járai, A. A. (2019) Edgeworth expansion with error estimates for power law shot noise. *Preprint:* https://arxiv.org/abs/1912.07275.

Kong, H.-B., Wang, P., Niyato, D., & Cheng, Y. (2018) Physical layer security in wireless networks with Ginibre point processes. *IEEE Transactions on Wireless Communcations* **17**(8), 5132–5147.

Lan, T., Sinkar, K., Kant, L. & Kerpez, K. (2010) Resource Allocation and Performance Study for LTE Networks Integrated with Femtocells. In *2010 IEEE Global Telecommunications Conference GLOBECOM 2010*, 1–6.

Last, G. & Penrose, M. (2017) *Lectures on the Poisson Process*. Cambridge University Press.

Lichte, H. S., Valentin, S. & Karl, H. (2010) Expected interference in wireless networks with geometric path loss: A closed-form approximation. *IEEE Communications Letters*, **14**(2), 130–132.

Parliament (2017) Telecommunications Sector Report. pages 1–22.
https://www.parliament.uk/documents/commons-committees/Exiting-the-European-Union/17-19/Sectoral%20Analyses/37-Telecommunications-Report.pdf [Accessed: September 2018].

SNS Telecom & IT (2018) Network complexity, 5G rollouts will drive SON (Self-Organizing Network) spending to $5.5 Billion. http://www.snstelecom.com/network-complexity-5g-rollouts-will-drive-son-self-organizing-network-spending-to-5-5-billion-says-sns-telecom-it [Accessed: September 2018].

Sousa, E. S. & Silvester, J. A. (1990) Optimum Transmission Ranges in a Direct-Sequence Spread-Spectrum Multihop Packet Radio Network. *IEEE Journal on Selected Areas in Communications*, **8**(5), 762–771.

Tall, A., Combes, R., Altman, Z. & Altman, E. (2014) Distributed coordination of self-organizing mechanisms in communication networks. *IEEE Transactions on Control of Network Systems*, **1**(4), 328–337.

Vaz, F., Sebastião, P., Gonçalves, L. & Correia, A. (2013) Femtocell deployment in LTE-A networks: A sustainability, economical and capacity analysis. *IEEE International Symposium on Personal, Indoor and Mobile Radio Communications, PIMRC*, 3423–3427.

Webster, S. (2015) Distributed heuristics for optimizing femtocell performance. MSc Thesis, University of Bath.

Win, M. Z., Pinto, P. C. & Shepp, L. A. (2009) A mathematical theory of network interference and its applications. *Proceedings of the IEEE* **97**(2), 205–230.

# A  Computational details

In this section we give the details of the computations for the general case of the asymptotic heuristic (32). We wish to compute the leading order asymptotic expression for the following multiple integral, in the limit of large $s$.

$$W_{k,s} := \int_{\rho^{-\gamma}}^{\frac{s}{k}} ... \int_{s_3}^{\frac{s-s_3}{s}} \frac{(s - s_2 - ... - s_k)^{-\frac{1}{\gamma}} - s^{-\frac{1}{\gamma}}}{(s - s_2 - ... - s_k)^{\frac{\gamma+2}{\gamma}} s_2^{\frac{\gamma+2}{\gamma}} ... s_k^{\frac{\gamma+2}{\gamma}}} ds_2 ... ds_k. \tag{A39}$$

In section 2 we defined a sequence of integrals $Q_k^{(j)}$ so that (A39) could be expressed concisely as

$$W_{k,s} = s^{-\frac{(2k+\gamma+1)}{\gamma}} \sum_{j=2}^{k} Q_k^{(j)}. \tag{A40}$$

The purpose of this Appendix is to compute the leading order term in $W_{k,s}$ and hence to justify (29).

We recall from section 2 the definition of the iterative sequence $Q_k^{(j)}$, (Definition 3), and compute $\sum_{j=2}^{k} Q_k^{(j)}$ in three steps:

(1). We find $Q_k^{(2)}$ in the cases where

    (a) $2 < \gamma < 4$,

    (b) $\gamma = 4$,

    (c) $\gamma > 4$.

(2). We find $Q_k^{(3)}$ in the cases where

    (a) $2 < \gamma < 4$,

    (b) $\gamma = 4$,

    (c) $\gamma > 4$.

(3). Finally we find $Q_k^{(j)}$ in the cases where

    (a) $2 < \gamma < 2(j-1)$,

    (b) $\gamma = 2(j-1)$,

    (c) $\gamma > 2(j-1)$.

A consequence will be that for all $\gamma > 2$, the dominant term in $\sum_{j=2}^{k} Q_k^{(j)}$ is $Q_k^{(2)}$.

**Step (1):**

We will begin by considering $Q_k^{(j)}$ in the special case where $j = 2$.

$$
\begin{aligned}
Q_2^{(2)} &= \int_{\frac{y_3}{1-y_3}}^{\frac{1}{2}} y_2^{-\frac{(\gamma+2)}{\gamma}} (1-y_2)^{\frac{-2-\gamma}{\gamma}} \left[(1-y_2)^{-\frac{1}{\gamma}} - 1\right] Q_1^{(2)} dy_2 \\
&= \int_0^{\frac{1}{2}} \frac{(1-y_2)^{-\frac{1}{\gamma}} - 1}{y_2^{\frac{\gamma+2}{\gamma}} (1-y_2)^{\frac{2+\gamma}{\gamma}}} dy_2 - \int_0^{\frac{y_3}{1-y_3}} \frac{(1-y_2)^{-\frac{1}{\gamma}} - 1}{y_2^{\frac{\gamma+2}{\gamma}} (1-y_2)^{\frac{2+\gamma}{\gamma}}} dy_2 \\
&= a(\gamma) - \int_0^{\frac{y_3}{1-y_3}} \frac{(1-y_2)^{-\frac{1}{\gamma}} - 1}{y_2^{\frac{\gamma+2}{\gamma}} (1-y_2)^{\frac{2+\gamma}{\gamma}}} dy_2 \\
&= a(\gamma) - \frac{1}{\gamma-2} y_3^{\frac{\gamma-2}{\gamma}} + O\left(y_3^{\frac{2\gamma-2}{\gamma}}\right)
\end{aligned}
\tag{A41}
$$

Therefore, using part (3) of Definition 3, we find that

$$
Q_3^{(2)} = \int_{\frac{y_4}{1-y_4}}^{\frac{1}{3}} \left[a(\gamma) y_3^{\frac{-\gamma-2}{\gamma}} - \frac{1}{(\gamma-2)} y_3^{\frac{-4}{\gamma}} + O\left(y_3^{\frac{\gamma-4}{\gamma}}\right)\right] dy_3.
\tag{A42}
$$

From (A42) we can see that there are three cases, distinguished by the value of $\gamma$, for which the form of $Q_3^{(2)}$ will be different. These are: $2 < \gamma < 4$, $\gamma = 4$, and $\gamma > 4$. Recall that we assume always that $\gamma > 2$ in order that the total signal strength at the origin remains finite almost surely. Using the iterative sequence in Definition 3, it is straightforward to compute $Q_k^{(2)}$ in each of these three cases.

**(1a):**

For $2 < \gamma < 4$.

$$
Q_3^{(2)} = a(\gamma) \frac{\gamma}{2} y_4^{-\frac{2}{\gamma}} + O\left(y_4^{\frac{\gamma-4}{\gamma}}\right)
$$

and from integrating this iteratively, using part (4) from Definition 3, we find that

$$
Q_k^{(2)} = a(\gamma) \left(\frac{\gamma}{2}\right)^{(k-2)} \frac{1}{(k-2)!} y_{k+1}^{-\frac{2(k-2)}{\gamma}} + O\left(y_{k+1}^{\frac{\gamma-2(k-1)}{\gamma}}\right),
\tag{A43}
$$

**(1b):**

For $\gamma = 4$,

$$
Q_3^{(2)} = a(4) 2 y_4^{-\frac{1}{2}} + \frac{1}{2} \log(y_4) + O(1)
$$

and from integrating this iteratively, using part (4) from Definition 3, we find that

$$
Q_k^{(2)} = a(4) \frac{2^{(k-2)}}{(k-2)!} y_{k+1}^{\frac{2-k}{2}} + \frac{2^{(k-4)}}{(k-3)!} \log(y_{k+1}) y_{k+1}^{\frac{3-k}{2}} + O\left(y_{k+1}^{\frac{3-k}{2}}\right),
\tag{A44}
$$

**(1c):**

For $\gamma > 4$

$$
Q_3^{(2)} = a(\gamma) \frac{\gamma}{2} y_4^{-\frac{2}{\gamma}} + O(1)
$$

and from integrating this iteratively, using part (4) from Definition 3, we find that

$$
Q_k^{(2)} = a(\gamma) \left(\frac{\gamma}{2}\right)^{(k-2)} \frac{1}{(k-2)!} y_{k+1}^{-\frac{2(k-2)}{\gamma}} + O\left(y_{k+1}^{\frac{6-2k}{\gamma}}\right).
\tag{A45}
$$

28

In (A44) we see that when $\gamma = 4$ a log term is introduced. However, in (10) we noticed that (when $k = 3$) this term cancels with the leading order term from $Q_k^{(3)}$. We will now compute $Q_k^{(j)}$ for $j \geq 3$ and show that log terms always either cancel or are of a lower order than existing terms and so can be disregarded. It will be convenient to introduce the exponent $\varepsilon = \min\left\{\frac{\gamma-2}{\gamma}, \frac{2}{\gamma}\right\}$, so that our error terms, apart from the log-term introduced when $\gamma = 4$, carry an extra power $y_{k+1}^{\varepsilon}$.

**Step (2):**

For $2 \leq l < j$ we refer to equation (2) of Definition 3. When $y_l$, $y_{l+1}$ are small, we use the approximation $(1 - y_l) = 1 + O(y_l)$ and $\frac{y_{l+1}}{(1-y_{l+1})} = y_{l+1} + O(y_{l+1}^2)$ to find that

$$Q_l^{(j)} = \left(\frac{\gamma}{2}\right)^{(l-1)} \frac{1}{(l-1)!} y_{l+1}^{-2(l-1)/\gamma} + O\left(y_{l+1}^{-2(l-2)/\gamma}\right). \tag{A46}$$

In order to find $Q_j^{(j)}$, equation (3) from Definition 3, we use the Taylor approximation to find that $\left[(1 - y_j)^{-\frac{1}{\gamma}} - 1\right] = \frac{1}{\gamma} y_j + O\left(y_j^2\right)$ and so

$$Q_j^{(j)} = \int_{\frac{y_{j+1}}{1-y_{j+1}}}^{\frac{1}{j}} \left(\frac{1}{\gamma} y_j^{-\frac{2}{\gamma}} + O\left(y_j^{\frac{\gamma-2}{\gamma}}\right)\right) Q_{j-1}^{(j)} dy_j. \tag{A47}$$

By setting $l = (j - 1)$ in (A46) and using this result in (A47) we obtain

$$Q_j^{(j)} = \int_{\frac{y_{j+1}}{1-y_{j+1}}}^{\frac{1}{j}} \frac{\gamma^{j-3}}{2^{(j-2)}(j-2)!} y_j^{\frac{-2(j-1)}{\gamma}} + O\left(y_j^{-\frac{2(j-2)}{\gamma}}\right) dy_j \tag{A48}$$

Let us now distinguish the cases $j = 3$ and $j \geq 4$. We first consider $j = 3$, and within this case, we consider separately whether $\gamma < 4$, $\gamma = 4$, or $\gamma > 4$.

**2(a):** $j = 3$ and $2 < \gamma < 4$. In this case, we have

$$Q_3^{(3)} = cy_4^{-\frac{4}{\gamma}+1} + O(1),$$

and iterating (4) of Definition 3 we get:

$$Q_k^{(3)} = O\left(y_{k+1}^{-\frac{2(k-1)}{\gamma}+1}\right) = O\left(y_{k+1}^{-\frac{2(k-2)}{\gamma}+\varepsilon}\right)$$

**2(b):** $j = 3$ and $\gamma = 4$. In this case, we have

$$Q_3^{(3)} = -\frac{1}{2} \log y_4 + O(1),$$

and iterating (4) of Definition 3 we get:

$$Q_k^{(3)} = -\frac{2^{(k-4)}}{(k-3)!} \log(y_{k+1}) y_{k+1}^{\frac{3-k}{2}} + O\left(y_{k+1}^{\frac{3-k}{2}}\right) = -\frac{2^{(k-4)}}{(k-3)!} \log(y_{k+1}) y_{k+1}^{\frac{3-k}{2}} + O\left(y_{k+1}^{\frac{2-k}{2}+\varepsilon}\right)$$

**2(c):** $j = 3$ and $\gamma > 4$. In this case, $Q_3^{(3)} = O(1)$, and iterating (4) of Definition 3 we get

$$Q_k^{(3)} = O\left(y_{k+1}^{-\frac{2(k-3)}{\gamma}}\right) = O\left(y_{k+1}^{-\frac{2(k-2)}{\gamma}+\varepsilon}\right)$$

29

**Step 3.** We now consider $j \geq 4$. We consider separately, whether $\gamma < 2(j-1)$, $\gamma = 2(j-1)$ or $\gamma > 2(j-1)$.

**3(a):** $j \geq 4$ and $2 < \gamma < 2(j-1)$. In this case $Q_j^{(j)} = O\left(y_{j+1}^{-\frac{2(j-1)}{\gamma}+1}\right)$, and the exponent of $y_{j+1}$ is negative. Therefore, iterating (4) of Definition 3 we get

$$Q_k^{(j)} = O\left(y_{k+1}^{-\frac{2(k-1)}{\gamma}+1}\right) = O\left(y_{k+1}^{-\frac{2(k-2)}{\gamma}+\varepsilon}\right).$$

**3(b):** $j \geq 4$ and $\gamma = 2(j-1)$. In this case $Q_j^{(j)} = O(\log y_{j+1})$. Therefore, iterating (4) of Definition 3 we get

$$Q_k^{(j)} = O\left((\log y_{k+1})\, y_{k+1}^{-\frac{2(k-j)}{\gamma}}\right) = O\left(y_{k+1}^{-\frac{2(k-2)}{\gamma}+\varepsilon}\right).$$

**3(c):** $j \geq 4$ and $\gamma > 2(j-1)$. In this case $Q_j^{(j)} = O(1)$, and we get

$$Q_k^{(j)} = O\left(y_{k+1}^{-\frac{2(k-j)}{\gamma}}\right) = O\left(y_{k+1}^{-\frac{2(k-2)}{\gamma}+\varepsilon}\right).$$

Therefore, we find that for all $\gamma > 2$ we have the required result:

$$\sum_{j=2}^{k} Q_k^{(j)} = a(\gamma)\frac{\gamma^{(k-2)}}{2^{(k-2)}(k-2)!}y_{k+1}^{\frac{-2(k-2)}{\gamma}} + O\left(y_{k+1}^{-\frac{2(k-2)}{\gamma}+\varepsilon}\right). \tag{A49}$$